MODELING TEMPERATURE-BASED VITICULTURE SUITABILITY FOR VINEYARD LOCATIONS IN THE FINGER LAKES

A Thesis
Presented to the Faculty of the Graduate School
of Cornell University
In Partial Fulfillment of the Requirements for the Degree of
Master of Science

by
Andrew Montreuil
January 2015

ABSTRACT

The Finger Lakes region of New York has garnered world-wide attention for its quality wines despite a climate that is barely suitable for viticulture. The complex terrain surrounding the Finger Lakes as well as the lakes themselves play a vital role in modifying the local microclimates to allow sustainable viticulture. By modeling these microclimates and quantifying the impact of the lake and terrain interactions, a vineyard-scale climatology dataset is created to assist in determining suitable and unsuitable locations for future viticulture operations.

BIOGRAPHICAL SKETCH

Andrew Montreuil graduated magna cum laude from the State University of New York (SUNY) at Oswego in 2007 with his Bachelors of Science in Meteorology with Honors. While at SUNY Oswego, Montreuil completed a two-year honor's thesis on how the general public perceives weather forecasts in addition to a department paper on the climatology of tornadoes in New York. Montreuil was awarded the Outstanding Senior Meteorology Student by the SUNY Oswego meteorology department.

Additionally, Montreuil runs a local weather forecasting company, Finger Lakes Weather and provides forecasts for both the general public and paying clients.

DEDICATION

This thesis is dedicated to my wife Maria for her loving support and gentle encouragement.

ACKNOWLEDGEMENTS

This work was supported by NOAA Contract EA133E07CN0090 and the NY State Agricultural Experiment Station.

The guidance and motivation received from Alan Lakso was greatly appreciated.

TABLE OF CONTENTS

Introduction

Background on Vineyard Site Selection

The Finger Lakes of upstate New York is an actively growing viticulture region with over 100 wineries established. This is the largest concentration of wineries in the United States east of California. These wineries play a very important role in the local economy, attracting tourists and providing jobs.

In 1987, the Wine Institute, a group focused on the economical and political promotion of American wines, declared the Finger Lakes Region an 'American Viticulture Area' (AVA). An AVA is a federally recognized region where viticulture is practiced successfully. Cayuga Lake was granted its own AVA within the larger Finger Lakes AVA in 1988, with Seneca Lake likewise getting its own AVA in 2003 (Wine Institute, 2010).

The climate of the Finger Lakes is classified as a "cool climate" environment for viticulture (Pagay and Cheng, 2010). This means that climate conditions are just barely suitable for the growth of good wine grapes. The climate of the Finger Lakes is more favorable for wine grape growth compared to other areas of Upstate New York largely due to the presence of the Finger Lakes, which act to modify the local climate (Newman, 1986).

The primary danger to viticulture in the Finger Lakes region is extreme cold temperatures during the winter season, which can kill both the grape vine and root stock. The New York Vineyard Site Evaluation System identifies temperatures of -24ºC and colder as damaging to all but the hardiest varieties of European wine grapes. Furthermore, the ability for a grape vine to withstand extreme winter cold temperatures

can vary depending on the condition of the plant and the weather prior to the extreme cold event (New York Vineyard Site Evaluation System, 2014).

Limitations of Current Knowledge on Vineyard Climatology

Due to the extremely complex terrain of the Finger Lakes region, temperatures can vary greatly over short distances. While modeling temperatures over complex terrain with an agricultural focus has been done in Korea (Chung et. al 2005), no such study has been completed in the Finger Lakes. Therefore, it is unknown which areas are suitable for viticulture, and which areas are too far away from the lakes to sustain viable viticulture.

Motivation

This study has been motivated by the seeming importance of the Finger Lakes on the local climate, especially during the winter months when temperatures might otherwise kill the root stock used for viticulture. It is hypothesized that the topography and lakes within the Finger Lakes region influence the temperature, preventing killing cold temperatures in the winter. By identifying areas where viticulture is climatologically suitable and unsuitable for viticulture, future vineyard owners can plan their operations for areas that will best suit viticulture.

Objectives

The objective of this study is therefore to identify areas that are climatologically suitable and unsuitable for viticulture through use of preexisting observational data and a geographically-driven climate model designed to predict the frequency of temperatures lower than the cold tolerance thresholds of a variety of grape species.

Methods

Study Site Description

The area of interest for this study will be the Finger Lakes region of Upstate New York, which encompasses all or parts of the following 10 counties (from west to east): Livingston, Steuben, Ontario, Yates, Schuyler, Seneca, Cayuga, Tompkins, Onondaga and Cortland. There are eleven lakes that comprise of the 'Finger Lakes. Each lake has a much longer north-south axis than east-west axis, making for long, narrow lakes.

With 173 km^2 of open surface water, Seneca Lake is the largest of all the Finger Lakes. It is also the deepest of the Finger Lakes, with a maximum depth of 188m, totaling 16km^3 of volume. The elevation of the lake is 136m above sea level. The south end of Seneca Lake is characterized by steep slopes leading to the lake's edge, while the northern end has much gentler slopes.

Within its AVA, Seneca Lake has nearly 50 independent vineyards (Fingerlakes.com, 2014). Many, but not all of the vineyards around Seneca Lake are located in proximity of the southern end of the lake on steeply sloping terrain. Because of this high number and availability of data from the Geneva Research Station, much of the focus of this study will be within the Seneca Lake area of the Finger Lakes Region AVA.

Temperature sensors were placed at the following vineyards: Fox Run Vineyards, along Route 14 between Penn Yan and Geneva on the west side of Seneca Lake; Red Tail Ridge, which is adjacent to Fox Run on Fox Run's southern border; Verill Vineyards, southwest of Ovid on the east side of Seneca Lake; Hazlitt wineries, located in the Town of Hector to the southeast of Seneca Lake; Glenora, located directly across

Seneca Lake to the west of Hector; King Ferry wineries in King Ferry; and the NYS Agricultural Experiment Station in Geneva, New York. For the purpose of this study, and also due to completeness of the record sets, 74 sensors from Fox Run, Red Tail Ridge, Verill, Hazlitt and Glenora were used (Figure 1).

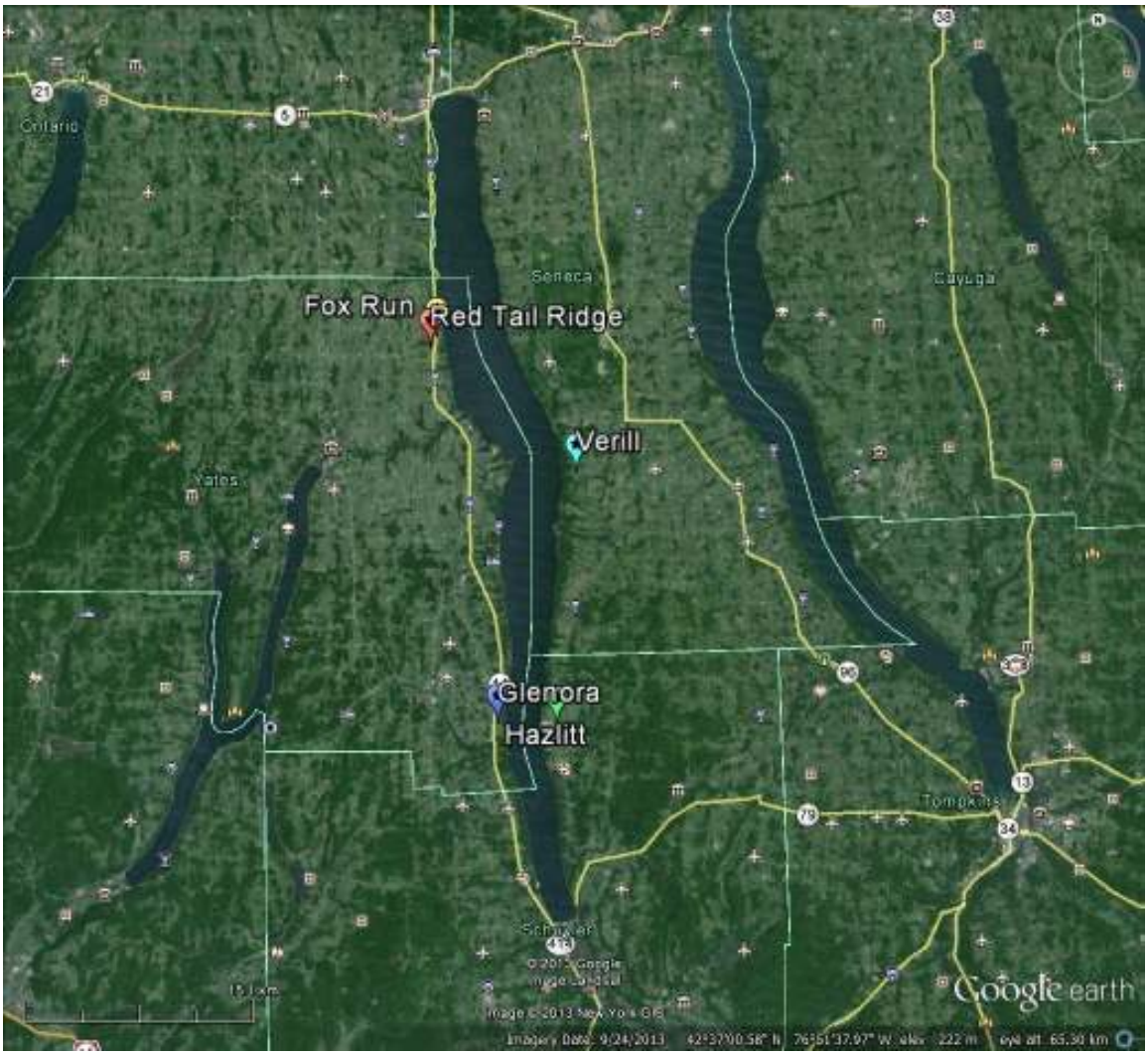

Figure 1- The locations of the five vineyards included in the study, all located in proximity to Seneca Lake.

Fox Run Vineyards is located 18km south of Geneva, NY along State Route 14. In all, 22 sensors were distributed among 4 distinct locations within the vineyard (Figure 2). However, two of the sensors, sensors FOX 23 and FOX 24, had short record sets and proved to be unreliable data sources. Three sensors, (Fox 2-4 on Figure 2) were

located directly west of the Fox Run Vineyards gift shop and restaurant on an open 6% slope falling to the east which eventually flattens out near the gift shop. These sensors ranged from 40m to 60m above lake level and were from 500m to 750m from the western shore of Seneca Lake. An additional eight sensors (Fox 5-14 on Figure 3) were located in a narrow, approximately 200m wide strip between tree lines, with another tree line on the northern half of the down slope, eastern edge. These sensors ranged from approximately 30m to 50m above lake level and were approximately 500m to 700m from the western shore of Seneca Lake. All of these sensors were located on the west side of Route 14.

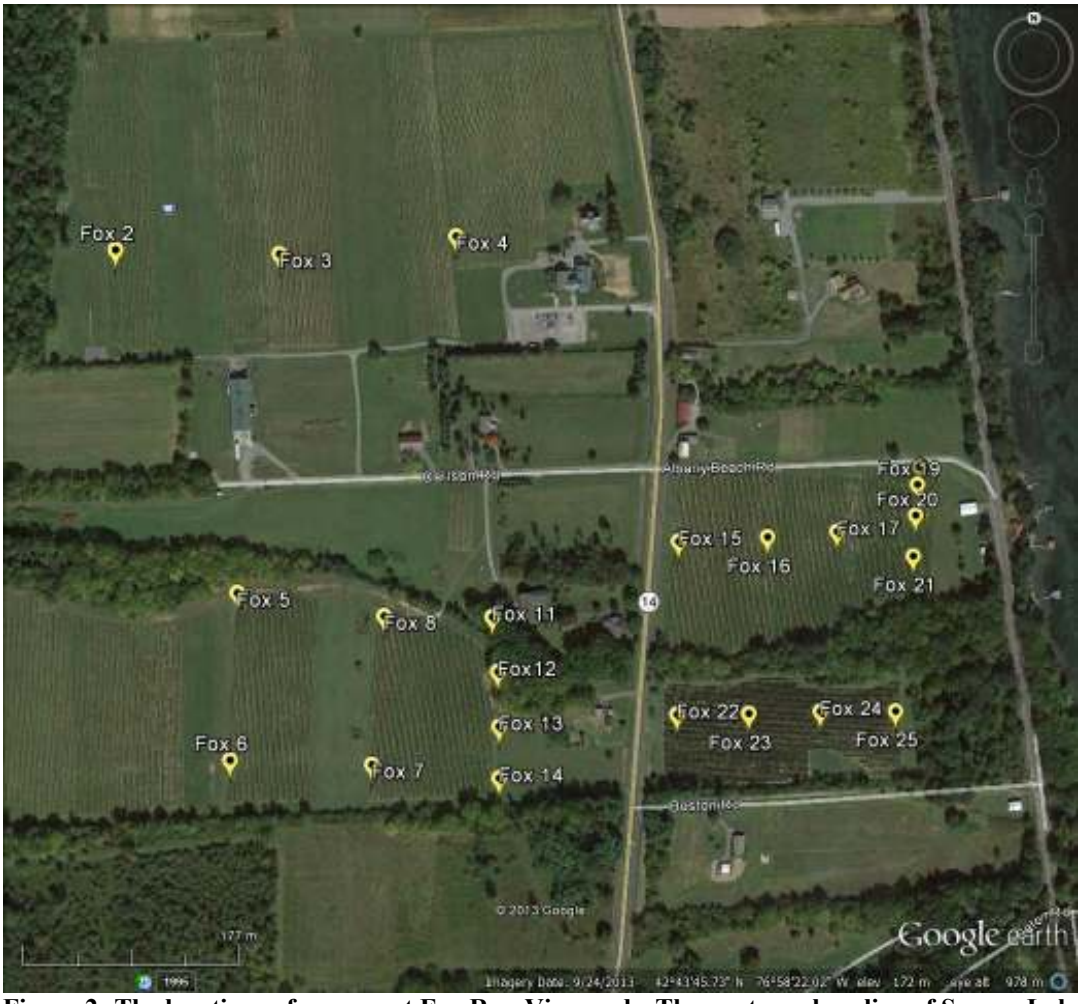

Figure 2- The locations of sensors at Fox Run Vineyards. The western shoreline of Seneca Lake can be seen on the right side of the image.

On the east side of Route 14, seven more sensors (Fox 15-21 on Figure 2) were located in a plot of land in close proximity of the Seneca Lake shoreline, with four of the sensors within 100m of the lake shore and no more than 10 to 15m above lake level. The other sensors were all within 330m of the lake shore and no more than 30m above lake level. Lastly, four sensors (Fox 22-25 on Figure 2) were located in a plot adjacent to the last mentioned plot, but with trees surrounding the plot on three sides. Only the upslope portion of the plot is open. This plot also is unique in that its rows on grape vines run parallel to the hillslope, oriented from west to east. All other plots with sensors have rows oriented north to south, perpendicular to the hillslope. Sensors were placed between 200m and 380m from the lake shore and were 20m to 30m above lake level.

Red Tail Ridge is located 1km south of Fox Run Vineyards (Figure 3). A total of ten sensors were placed in two distinct locations at Red Tail Ridge. All sensors were on the west side of Route 14. Four sensors (RTR 91-94 on Figure 3) were located on a steep slope, averaging between 10-20% slope gradient. This strip of land is approximately 110m wide with a forest to the north and a tree line to the south. These sensors range from 670m to 900m from the shore of Seneca Lake to the east and are 40m to 60m above lake level. The other six sensors (RTR 95-100 on Figure 3) were located in a wide, open plot directly upslope from the first five sensors. A forest was located to the north of this plot. This plot has a gentle slope gradient between 2% and 4%. At some sensor locations, the slope aspect is to the northeast instead of due east. These sensors ranged from 900m to 1125m from the shore of Seneca Lake and are 60m to 70m above lake level. One of these sensors, RTR 96, was near the edge of a small pond.

Figure 3- The location of sensors at Red Tail Ridge. Notice the close proximity of Fox Run Vineyards to the north.

A dense plot of sixteen sensors was placed at the Verill vineyard, about 4 km southwest of Ovid in southern Seneca County (Figure 4). All sensors were in a single 10.2 hectare field. At its closest, this plot ranged from 800m to 1100 m from the east shore of Seneca Lake. The elevations of the sensors were all between 70-90m above lake level. The area immediately surrounding this field is mostly open with few trees. The slope gradient in this plot descends from east to west at a fairly consistent 6%. There are also some localized north-south oriented hillslope undulations.

Figure 4- The location of sensors at Verill Wineries near Ovid, NY. The inset picture shows the distance of the sensors from eastern shore of Seneca Lake to the west.

The sensors were mostly arranged in two north-south rows, with an intersecting row of west-east sensors. The two rows were located at the western edge of the field, where some local topographical undulations were observed. The intersecting west-east column extended from the western to eastern edge of the field and was located in the center of the field relative to north and south. Six sensors (VER 26-29, 32, 38 on Figure 4) were located in this column, with two of the sensors (VER 32 & 38) also being included in the aforementioned rows.

The Glenora Winery vineyard with sensors is located just north of the winery, or about 5km southeast of the town of Dundee in southeastern Yates County (Figure 5). The sensors here range from 330m to 750m away from the western shore of Seneca Lake. A total of nine sensors were placed in this field in a west to east transect, which is the same direction as the slope aspect. This transect is broken into two parts, an upper and a lower transect. Two sensors (GLN 130 & 131 on Figure 5) are aligned on the same elevation contour. One of these sensors (GLN 130) marks the down slope end of the upper section, while the second (GLN 131) marks the down slope beginning of the lower section.

Figure 5- The location of sensors at Glenora Wineries (western shoreline of Seneca Lake shown on right).

The upper section can further be divided into three main areas of varying slope gradient. Initially, the slope gradient is fairly steady at about 13%. Then, the slope decreases to about 7% before sharply increasing to nearly 20% near sensor GLN 130. It is also critical to note that immediately down slope of GLN130 is a tree line. The four sensors in this upper transect (GLN 126-130 on Figure 5) range from about 760m to 450m from the shore of Seneca Lake and vary from 95m to 200m above lake level in elevation. The lower transect has five tightly clustered sensors along a hillslope of approximately 10% slope gradient. These sensors (GLN 131-135 on Figure 5) range from 450m to 340m from the lake and are 75m to 100m above the lake level.

Lastly, a collection of sensors was placed in a number of plots at the Hazlitt Wineries in Hector, NY. These sensors are classified into two sets: Lower Hazlitt, which includes all sensors west of NY 414 (Figure 6); and Upper Hazlitt, in which all sensors are east of NY 414 (Figure 7). The distinction is made because the two sets are separated by more than 800m at their closest, and by nearly 2500m at their farthest.

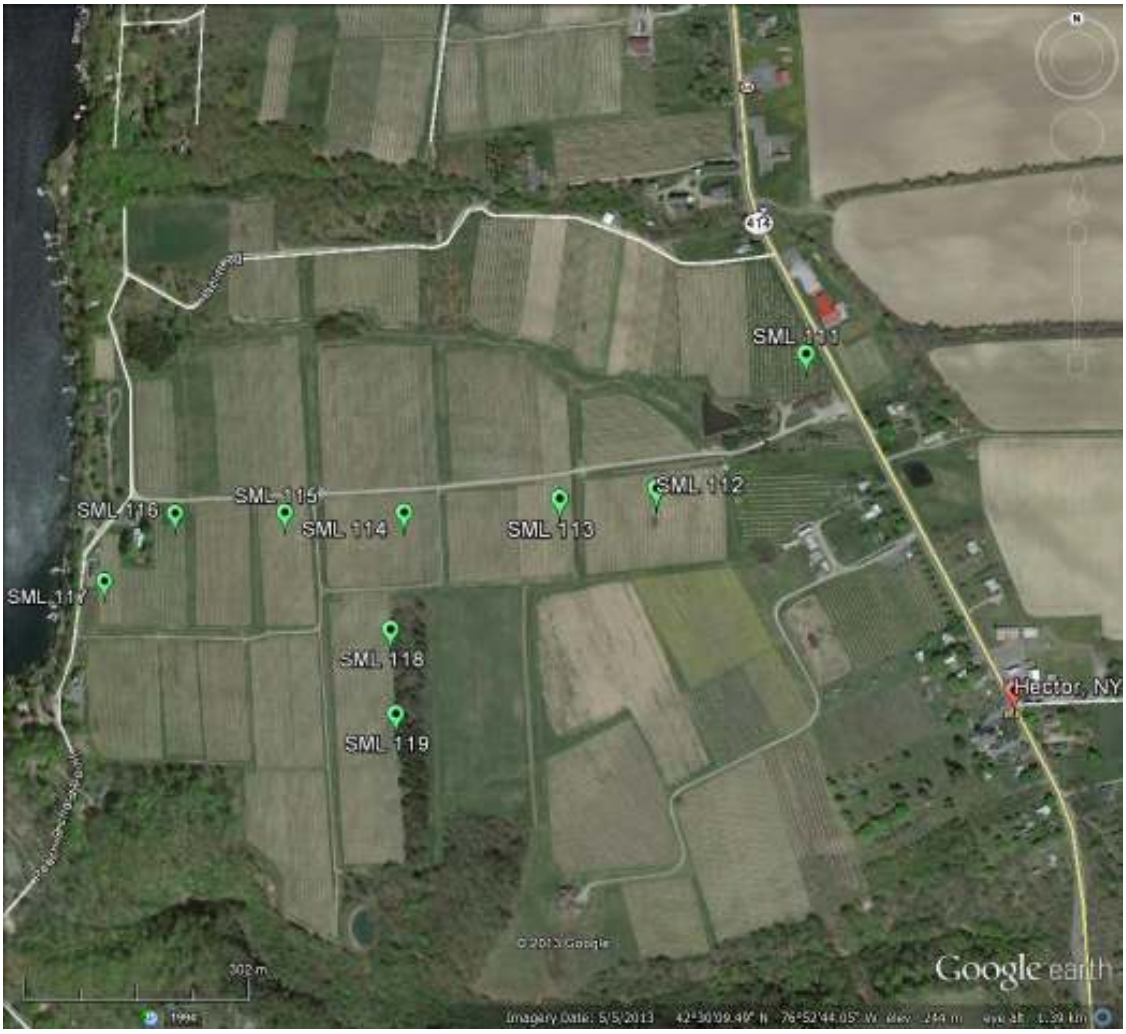

Figure 6- The location of sensors at lower Hazlitt. The center of Hector, NY has been marked for reference with Figure 7.

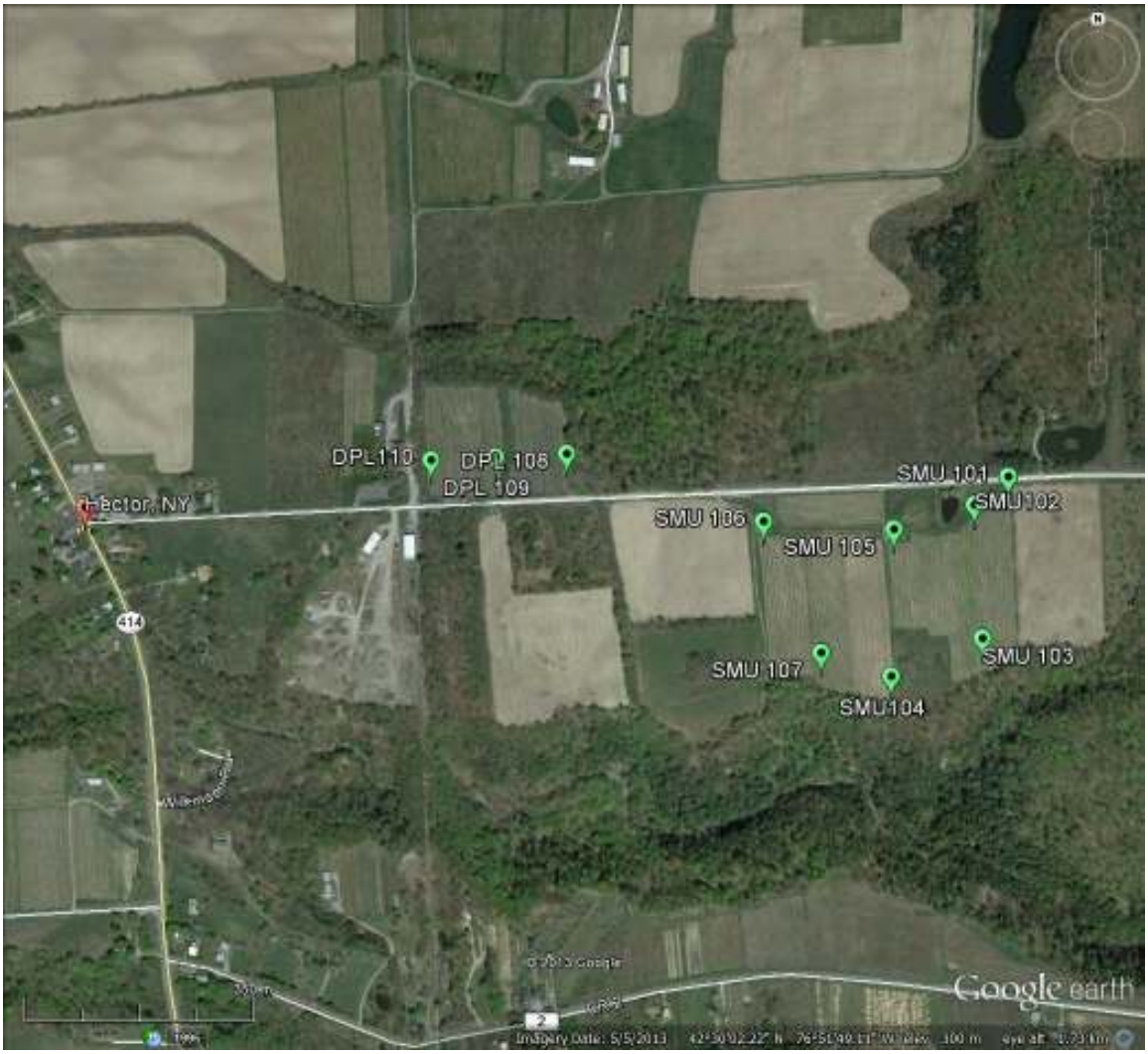

Figure 7- The location of sensors at upper Hazlitt. The center of Hector, NY has been marked for reference with Figure 6.

The sensors at Lower Hazlitt were generally placed in open fields on a steep hillslope, most with no tree influence. One sensor (SML 111 on Figure 6) was actually placed in an orchard instead of a vineyard, while two others were immediately down slope of a narrow tree line (SML 118 and 119 on Figure 6). The remaining six sensors were arranged to form a transect from the top of the hillslope to the lake shore. As such, the closest sensor (SML 117) is a mere 63m from the lake shore and 13m above lake level. The sensor at the top of this transect (SML 111) is about 750m inland and 113m

above sea level. The hillslope along this transect is somewhat undulating, but averages about 14.8%.

The sensors at Upper Hazlitt (Figure 7) can be further split into two distinct sections. The first of these contains three sensors (SPL 108-110 on Figure 7) in an east-west down slope line. The average slope gradient along these three sensors is about 15%, but has a maximum of nearly 23%. When continuing down slope beyond these sensors, the land flattens with a 5% or less slope gradient. These three sensors range from 1700m to 1900m from the east shore of Seneca Lake and are 150m to 165m above lake level. Trees can be found on the north side of the plot, with a forest immediately east (upslope) from the sensors. The other seven sensors (SMU 101-107 on Figure 6) were in a plot with a less typical hillslope than the other plots in the study. This plot has a variety of undulations and pockets, but generally slopes in a southwesterly direction. Immediately southwest of the sensors is a forested gulley with a small stream that flows down to Seneca Lake. These sensors range from 2200m to 2550m from the lake shore and are 175m to as much as 190m above lake level.

Data Set Descriptions

The observational data from the aforementioned temperature sensors were obtained from Dr. Alan Lakso and Richard Piccioni of the Department of Horticultural Sciences at the New York State Agricultural Experiment Station in Geneva, New York. These data were recorded using iButton 1-Wire Thermochron (DS1921G) sensors. The sensors were placed in a double PVC radiation shield. This shield consisted of two sizes of PVC pipe being cut length-wise, and then layered together so a small gap existed between the two PVC layers. The iButton sensor was then attached on the

inside of the smaller PVC pipe, equidistant from the edges of the PVC and the bottom of the PVC (Figure 8). Temperature data were recorded every 30 minutes from January 2006-June 2011, with the exception of November 29, 2010 to December 21, 2010, for which no data are available for unknown reasons.

Figure 8- iButton sensor with PVC radiation shield on wire in vineyard amongst grape foliage.

Sensors were placed in vineyards around Seneca and Cayuga Lakes. The density of sensors in participating vineyards ranged from 0.3 sensors per hectare to 2.38 sensors per hectare. Sensors were typically located in either a grid format or along transects. Sensors were placed on preexisting terracing wires used to support the grape vines. Sensors were placed on wires approximately 1.5-2 meters from ground level. Since sensors were on the grape vine wires, most sensors were surrounded by foliage during the growing season. Vineyard workers also sometimes inadvertently would move, knock down, or even destroy sensors during normal viticulture operations. Such sensors were replaced or returned to their original location.

Each sensor recorded temperatures instantaneously at 30 minute intervals and could store up to 40 days of data. Therefore, it was necessary for the data to be manually downloaded each month using a handheld computer, which was done by Richard Piccioni. These raw data were then sent to the Institute for the Application of Geospatial Technologies in Auburn, NY, for data compilation. Each observation contained the time of the observation and the temperature reading (ºC) to the nearest 0.5ºC, and the sensor ID number.

The location and elevation of each sensor was surveyed in October and November 2011 with a handheld Trimble GPS. A set of 50 points was collected for each sensor location, which were then differentially corrected by to ensure accuracy. Differential correction is a process to increase the accuracy of GPS data by comparing GPS recordings with the actual, known location of a control point. By knowing the noise errors at the known location, those errors can be applied to nearby GPS readings at unknown locations, such as the handheld unit used to survey the sensors. By taking 50 readings at each sensor, the locations and errors could be averaged, thus increasing the accuracy. Accuracy estimates placed 88.3% of the readings within 1 meter of their differentially corrected location.

To supplement the Lakso dataset, data from the North American Regional Reanalysis project, referred to as NARR henceforth, was also used (National Center for Environmental Protection, 2007). This is a “long-term, consistent, high-resolution climate dataset” that was used as the basis for this project’s climatology. This dataset was created to give a snapshot of the weather every three hours stretching back to

1979 and was compiled from a wide variety of sources, including archived observataional, radar, satellite and weather model data.

With a grid spacing of 32km, all five vineyards with Lakso data were contained with a single grid cell, centered at 42.632181 N and 76.861858 W. Incidentally, this is about 2km south of the Verill vineyard. The grid cell elevation is 276.8 m, which is above almost all the Lakso sensors except SMU 101-107 and DPL 108-110, located at the Hazlitt vineyards. The data from this 32 km grid was down sampled to a 10m grid. This was done to compare the variables with the sensor data and also to coincide with a standard 10m digital elevation model.

Several variables from the NARR dataset were used. Temperature data were selected at 2m and 30m and at 950 hPa and 975 hPa. The temperature data were in degrees Kelvin and converted to both Celsius and Fahrenheit as needed. Total cloud cover was obtained as a percent of the sky obscured by clouds. Wind speeds in the *u* and *v* directions, that is the north-south components and east-west components of the wind, at 10m were also used with velocity units of ms^{-1}. All of these variables were available during the time span from January 1, 2006 to June 15, 2011 to match the period of reliable Lakso sensor data with only sporadic missing data for some hours. Each variable's data were available at 3-hour increments, starting with 00 Coordinated Universal Time (UTC) each day.

Analytical Methods

1) Exploratory Analysis

Before any analysis could be done on the Lakso data set, it was necessary to properly reformat and conduct quality control on the data. When received, data for each

sensor was in its own file with no chronological ordering. Additionally, some records were duplicated and others were erroneous.

The first procedure was to remove any values outside of the climatological norms for the Finger Lakes region. Mostly, this applied to temperature readings that were erroneously high, on the order of 50º C or higher. Many of the values that were removed were recorded as 85º C, which was an indication that the data download had, at some point, been interrupted when taking the data from the sensor to the computer.

The last quality control and formatting step was to arrange all observations from a given vineyard into a single file. A computer program was created to arrange all the observations at a given time in a vineyard into a single record. Within this process, sensors that had multiple observations for a single time were compared to other sensors at the same time, and the most similar observation was kept. Thus, a collection of lines was created, each specifying a single time. These records were then sorted into chronological order. A value of -999 was used to designate missing data.

To initially examine the data and assess sensor-to-sensor and vineyard-to-vineyard differences, a number of simple analyses were conducting by plotting sensor data using Google Earth. First, the sensors coordinates were input into Google Earth using the latitude and longitude values obtained from the GPS survey. These coordinates were checked visually using Google Earth's satellite capabilities to ensure accuracy. Once the sensor locations were confirmed, additional plots could be created by 'dropping' pins with the analysis value on the sensor locations. Color coding was also used to aid in the visualization of data. Python programs were created to obtain the data for the various analyses.

The first analysis was the coldest temperature recorded by each sensor over the sensor record. A mean and standard deviation were computed from these absolute minimum temperatures, and sensor values were color coded by the number of standard deviations from the mean. Two sensors were over 2 standard deviations below the mean: SMU 107, with a minimum temperature of -27.5º C (Figure 9) and RTR 96, with a minimum temperature of -27.0º C (Figure 10). With the exception of FOX 14, all the sensors that were between 1 and 2 standard deviations below the mean were located at Red Tail Ridge and Hazlitt, the location of the aforementioned two coldest sensors as well.

Figure 1- Sensors 101-107 at Hazlitt with coldest recorded temperature in Celsius and color coded by standard deviations from the mean coldest temperature across all sensors. Note that SMU 107, colored in pink, recorded the coldest temperature at -27.5ºC.

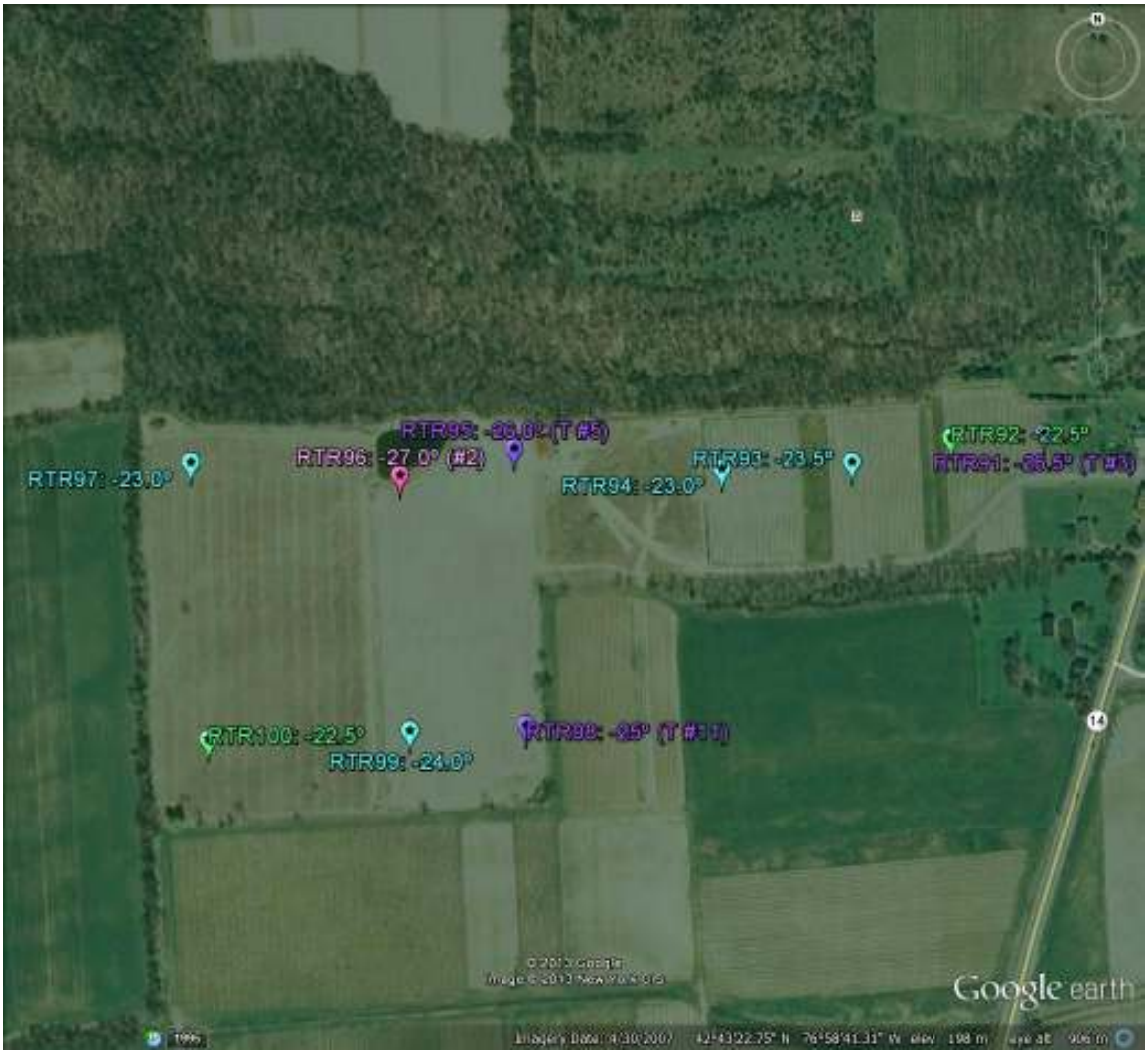

Figure 2- Sensors 91-100 at Red Tail Ridge with coldest recorded temperature in Celsius and color coded by standard deviations from the mean coldest temperature across all sensors. Note that RTR 96, colored in pink, recorded the second coldest temperature at -27.0ºC.

All winter night minimum temperatures, defined as the coldest temperature between 0600 UTC and 1200 UTC, for a sensor were then averaged. The 10 coldest winter nights were plotted along with the coldest values at each vineyard. The sensor with the coldest average minimum winter temperatures was GLN 130, the aforementioned tree line sensor. The second and third coldest nights were sensors FOX 11 and FOX 12, both of which also have influence from tree lines (Figure 11). Likewise,

the fourth, fifth and sixth coldest sensors were SMU 104, 107 and 105- all with trees immediate down slope of the sensor. The eight and ninth coldest sensors were SML 118 and 119, both of which had trees immediately upslope of the sensors. The coldest sensor at Red Tail Ridge was RTR 91, which ranked 14th and at Verill was VER 26, which ranked 29th. The same analysis was conducted with summer night-time temperatures using the same UTC time period. The only sensors that ranked in the top 10 in both winter and summer were sensors SMU 103, 104 and 107.

Figure 3- Sensors 5-14 at Fox Run. Sensors 11, 12 and 14 are specially marked for having average winter minimums ranking within the top 10 coldest among all sensors.

In order to get a sense for which sensors were coldest overall, a number of different measures of cold needed to be taken into account. For comparison, the sensors were ranked from coldest to warmest in five different categories. Therefore, the coldest sensor got a score of 1, and the warmest a score of 74, since there are 74 sensors. The scores for each of the five categories were summed to obtain an overall score. The scores were then ranked from the smallest sum to the largest. Therefore, the sensor ranked #1 could be considered the coldest, and the sensor ranked #74 the warmest. The five categories that were evaluated were: the lowest recorded temperature at the sensor, the average winter daily minimum temperatures, the number of recorded temperatures of -20ºC or lower, and the temperature at 1200 UTC on two case study days: a radiational cooling night (Feb 23, 2011) and the sensor temperature on the coldest night (January 25, 2011), as calculated by the average minimum temperature across all sensors.

Two sensors tied for the lowest overall score- RTR 95 and RTR 96, two adjacent sensors at Red Tail Ridge. It is also interesting to note that three other adjacent sensors- RTR 94, RTR 98 and RTR 99 also ranked in the top-10 (Figure 12). The area around these sensors is characterized by steeper slopes uphill and downhill from the sensors, but an under 5% slope gradient in the area of the sensors. Additionally, at sensors RTR 95 and RTR 96, there is a diagonal hillslope to the northeast, towards a tree line and gully. It can be hypothesized that cold air draining from uphill locations pools in this area of lesser slope gradient and tree line influences, possibly leading to a local minimum in temperatures.

Figure 4- Sensors 91-100 at Red Tail Ridge with 'cold score' ranks. Note sensors 95 and 96 tied for the coldest overall rank among all sensors, while 94, 98 and 99 all ranked in the top 10 coldest.

A second collection of adjacent sensors were also ranked within the top 10: SMU 102, SMU 103, SMU 104 and SMU 107, at the Hazlitt Vineyards (Figure 13). Among these sensors, SMU 107 was the coldest of all tested sensors except the top ranking RTR 95 and RTR 96. These sensors are at high elevations, far from the lake, and also have some tree line influence, especially at SMU 107. Here, the slope aspect is to the west-southwest and intersects a tree line almost perpendicularly, possibly leading to the accumulation of cold air.

Figure 5- Sensors 101-107 at Hazlitt with 'cold score' ranks. Note sensor 107 is the third coldest overall rank among all sensors, while 102, 103 and 104 all ranked in the top 10 coldest.

In contrast, the sensors that ranked as the highest numbers can be assumed to have the warmest temperatures during winter nights. The top two sensors, ranked #74 and #73, were also located at Hazlitt- sensors SML 116 and 117. These two sensors were located near the shore of Seneca Lake and had no influence from tree lines or changing slopes. Nearby sensors also were very warm, with sensor SML 114 tying for 68th, SML 115 ranking 65th, and SML 119 ranking 62nd (Figure 14). Most of the other 'warm' sensors were located at the Verill vineyard, with many sensors ranking in the

50s, 60s and 70s. These rankings seem to be in line with the other analyses that were done. It can be hypothesized that many warm sensors are located at Verill due the absence of any tree lines or frost pockets to trap cold air.

Figure 6- Sensors 114-119 at Hazlitt with 'cold score' ranks. Note sensors 116 is ranked 74th among 74 sensors, which can be interpreted as the warmest sensor. Sensors 114, 115 and 117 also all ranked within the top 10 warmest sensors.

In order to achieve project goals, it was necessary to develop a relationship between the Lakso sensor data and the NARR dataset. It was hoped that a relationship could be derived that would adjust the NARR temperatures to closely represent the

sensor temperatures, especially during extremely cold nights, which pose a threat to the grape vines. This relationship could then be applied over the duration of the NARR data set to create the desired climatology of killing winter cold.

2) Lake Index

Considering the topography of the land surrounding the Finger Lakes, and that the depth of the lakes typically prevents the lakes from freezing, it is important to take into consideration how the lakes may influence the cold air drainage of the region. While cold air flows downslope towards the lake, it can be assumed that the lake can modify the air over it and spread inland, counteracting the cold air drainage.

Previous, in-house research was conducted at the Northeast Regional Climate Center (NRCC) on the influence of Seneca Lake on the air temperature of the surrounding area. This research indicated that the amount of warming from the lake on a winter radiational cooling night was a function of the elevation above the lake and the horizontal distance to the lake shore. The elevation and distance to the lake represent the two sides of a right triangle. If the area of this triangle for a given location near Seneca Lake is less than 25,000 m^2, that location was assumed to be warmed by the lake.

A simple analysis was conducted to verify this research and formulate an equation, which could be used to account for the warming influence of the lake at a given location. The basis of this analysis was the physical mixing of warm, lake-modified air and cool, downslope flowing air from uplands. This was calculated by a mass-weighted average of the temperatures of the air above the lake and the land. For the purposes of simplicity and due to a lack of data, two assumptions were made.

First, the temperature of Seneca Lake, and thus the air in contact with the water, was always assumed to be 1°C. This was assumed because Seneca Lake does not freeze during the winter months due to its depth, but remains just above freezing. This assumption was validated by a Navy research project on Seneca Lake in the 1970s that took some surface water temperature readings during the winter months (Fliegel 1973). This assumption was made because there are no long term average daily or monthly surface water temperature data available for Seneca Lake or other Finger Lakes.

Second, the temperature at the top of the air was assumed to be modified by the lake and the mass of said air was calculated. If a temperature inversion was present in the NARR data, the temperature and height of the NARR level at the top of the inversion was used. This inversion temperature was calculated by comparing the temperature from the NARR at 25mb intervals of increasing height until a decrease in temperature from one height level to the next was observed. If no inversion was present, the temperature and height of the NARR surface pressure were used, as this was always at a higher level than the lake surface due to the NARR grid characteristics. The average of this temperature and the 1°C lake-surface air temperature were used to characterize the temperature of the volume of air over the lake. The height of the top of the inversion was used in combination with half of the width of Seneca Lake, along with the density of the average air at its given temperature, to calculate the mass of the volume of air above the lake that would be mixed. The width of Seneca Lake was estimated using Google Earth, with a half-width value of 2100m used for Fox Run and Red Tail Ridge, 1700m for Verill and 1150m for Hazlitt and Glenora. These assumptions were made due to a lack of observed boundary layer data from the Finger Lakes area.

The area of the triangle from the aforementioned NRCC process was used to calculate the mass of the colder air originating over the land to mix. This was calculated for a given sensor location by using the triangular area from the sensor's elevation above the lake and distance from the shore, converting this area to a unit volume (i.e. by multiplying it by 1m) and accounting for the density of the air at its temperature. The temperature of this air was assumed to be the NARR temperature. It was assumed that the entire mass of air over land would mix completely with the entire mass of air over the lake (Figure 18). These assumptions were made for simplicity and to be able to use the methodology over the entire NARR dataset, extending back to 1979.

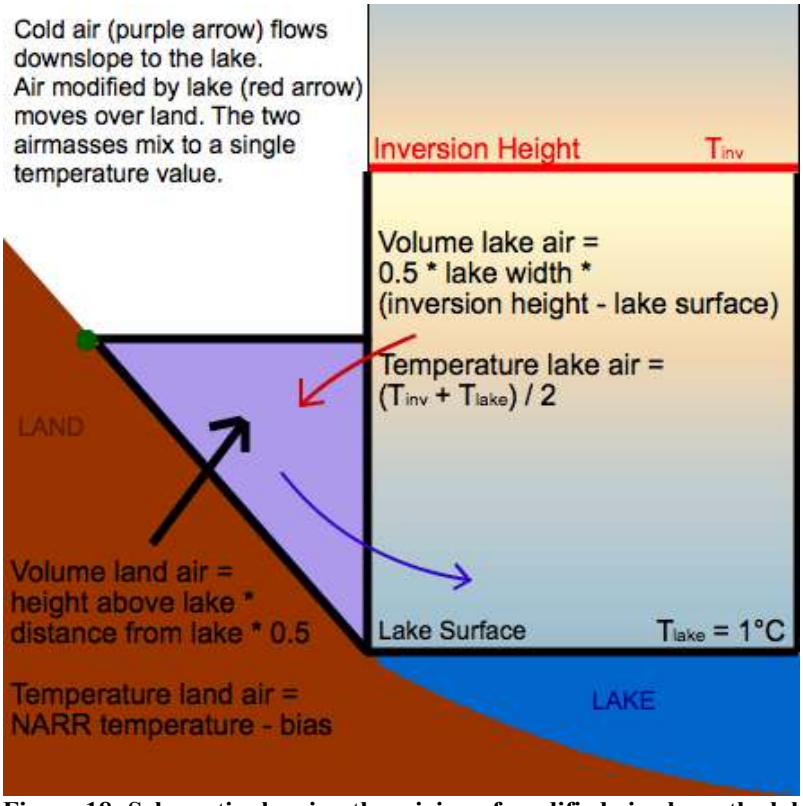

Figure 18- Schematic showing the mixing of modified air above the lake and colder air over land.

To test the NRCC conjecture that Seneca Lake has an influence on volumes of air up to 25,000 m^3, and to determine which sensors should ultimately be adjusted to

account for lake influence, the above assumptions were used with a simple mass-weighted averaging analysis over all NARR minimum temperatures during the study period. The change in temperature from mixing was recorded for each minimum and categorized by the original NARR temperature. These temperature categories were chosen so that at least 20 observations were in each category. Categories had a range of every 3°C for values between +6°C and -15°C, with additional categories for values warmer than +6°C and colder than -15°C. These categories were made under the hypothesis that the ultimate change in temperature from mixing would vary based on the initial NARR temperature.

Figure 19 shows the results of this analysis, with each data point representing the median temperature change from mixing at a given volume for that temperature category. Trend lines were added to each temperature category, with the equation and r-squared value displayed on the map. The maximum influence from the lake occurs on the coldest NARR minimums at small land air volumes, i.e. at sensors very close to the lake. The amount of temperature change decreases both as the NARR warms and as the volume increases, as was expected.

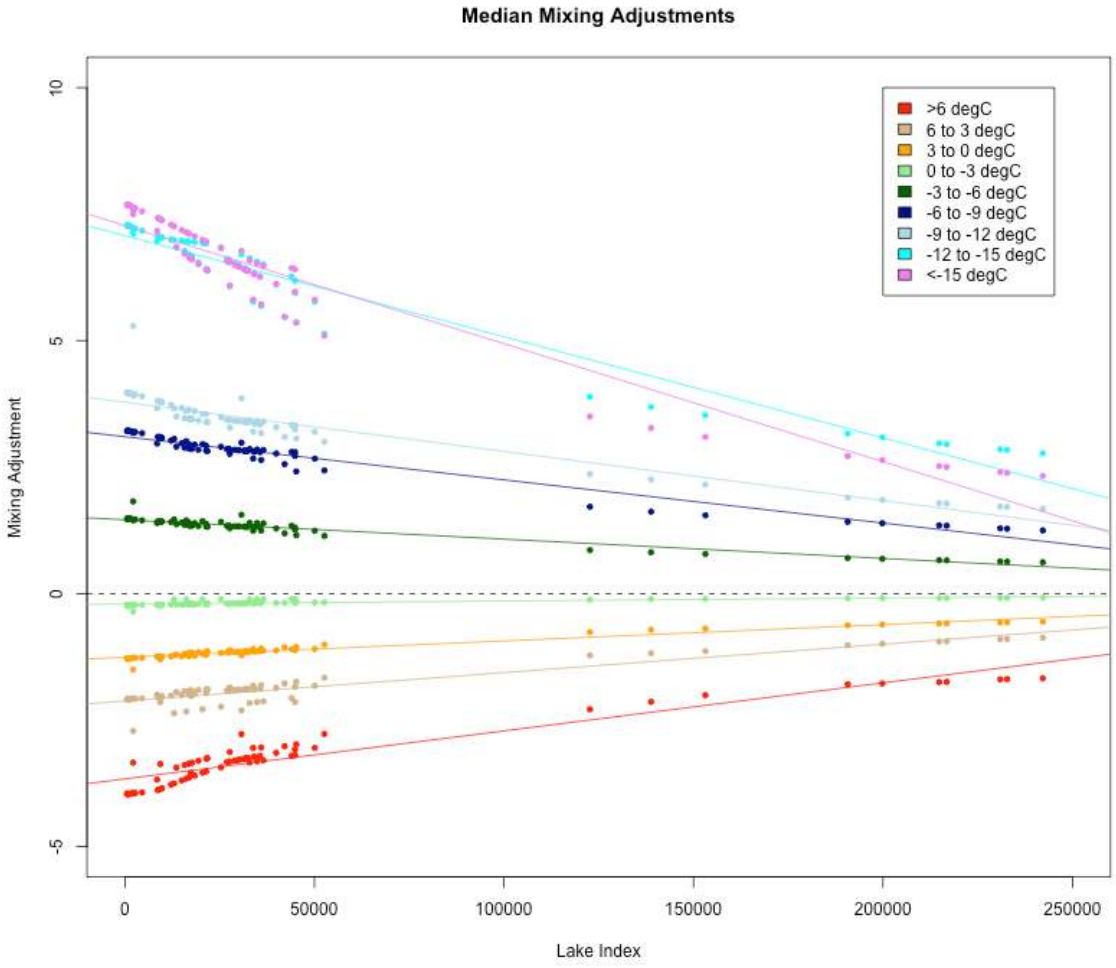

Figure 19- Median change in temperature due to mixing with lake air at different volumes of land air and at different temperature ranges. Each data point represents the adjustment applied to a given sensor.

While a linear trend line was used, it is also apparent that as the volume increases, the amount of temperature change does not change linearly, but instead flattens off towards an asymptote unique to that temperature category. The approximate point of inflection of this trend was determined to be around 40,000 m^3 and this value was chosen as the cut off for lake influence, instead of the 25,000 m^3 the NRCC concluded. Figure 20 shows the same analysis, but only for sensors within this 40,000 m^3 volume. One additional step was also taken for this plot: the median temperature

change from mixing at sensors with a volume greater than 40,000 m^3 was subtracted from each data point to remove noise, since in Figure 19 even volumes above 40,000 m^3 showed temperature changes. The equations shown on Table 2 were used to further adjust those locations within the area of lake influence.

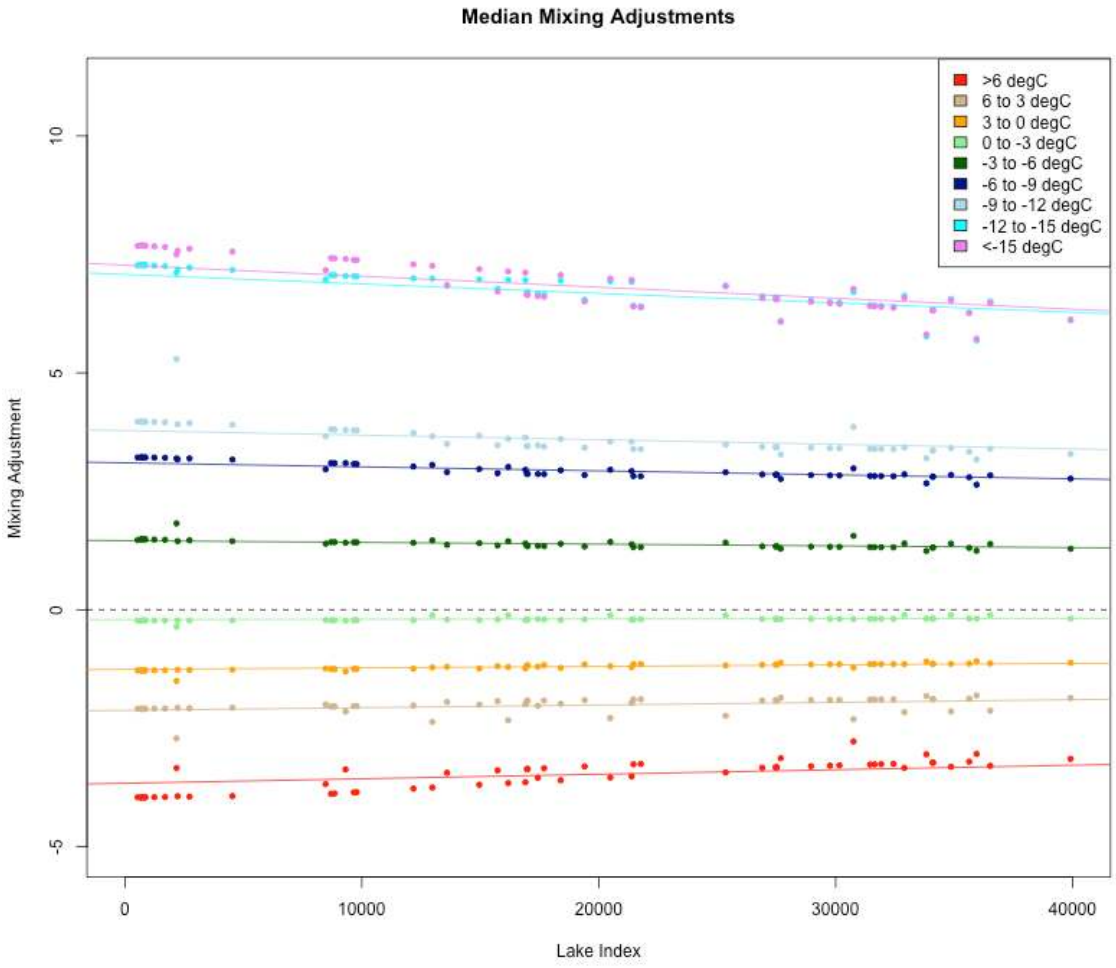

Figure 20- Median change in temperature due to mixing with lake air at different volumes of land air and at different temperature ranges. The equations listed in Table 1 (below) were derived from this plot and used to account for lake influence for the remainder of the study.

Table 1- Equations of trend lines in Figure 20. These equations were used to adjust the temperature of the air near the lake, with x representing the lake index value representing combined height above and distance from the lake surface.

Temperature Range [°C]	Adjustment Equation	R-Squared Value
> 6°	$2.3e^{-5}$ x – 1.65	0.81
6° to 3°	$0.4e^{-5}$ x – 0.85	0.17
3° to 0°	$0.4e^{-5}$ x – 0.57	0.85
0° to -3°	$0.2e^{-5}$ x – 0.12	0.31
-3° to -6°	$-0.4e^{-5}$ x + 0.59	0.55
-6° to -9°	$-1.2e^{-5}$ x + 1.45	0.83
-9° to -12°	$-1.8e^{-5}$ x + 1.53	0.79
-12° to -15°	$-2.9e^{-5}$ x + 2.54	0.79
< -15°	$-4.2e^{-5}$ x + 4.47	0.85

3) Sensors Minima vs NARR Minima at All Sensors

Research conducted by Chung et. al (2005) modeled cold air drainage for agricultural applications by creating a model of cold air accumulation over complex terrain in South Korea. These investigators accounted for varying elevations by using a lapse rate correction and a geographic information system (GIS) to locate cold air basins. A similar approach was adapted for this project.

Based on the exploratory analysis of the Lakso dataset, it was hypothesized that the primary influence on the temperatures of the sensors during winter nights is related to cold air drainage with some influence from Seneca Lake. Since cold air drainage is maximized under radiational cooling conditions, the influence of the different aspects of radiational cooling needed to be tested. By isolating a variable or variables that seemed to indicate a radiational cooling night, a relationship between the NARR and Lakso sensors could be developed. A series of boxplots was created to identify these influences and to make an appropriate adjustment.

Additionally, a GIS was utilized to visualize the air drainage fields and accumulation of cold air over the study area in an attempt to further identify factors that

may result in a systematic difference between the NARR and sensor temperatures. If a relationship is apparent between the Lakso data, air drainage and weather conditions provided by the NARR dataset, a predictive model could be developed and applied using the NARR dataset to create a climate-based suitability map for viticulture in the Finger Lakes region.

Since the primary concern of this study is killing winter cold, the first set of boxplots were created to show the differences between the minimum temperatures at each sensor and the NARR minimum temperature for the corresponding day. These differences were compiled for each day in January, February, March and December for 2006-2011, not including December 2011 which, as previously mentioned, has no sensor data.

Two additional preliminary analyses were also conducted that closely relate to the first. One of these analyses used only the fifty coldest minimums at each sensor, while the other used the fifty coldest NARR minimums. These two sets of boxplots show the differences in minimum temperatures when the nights are at their coldest. Fifty minima were chosen to represent slightly less than 10% of available nights for analysis.

All three sets of boxplots show the differences at each sensor, with all sensors within a vineyard shown on a single plot. This allows for analysis between individual sensors that are in close proximity to one another in an attempt to highlight potential differences between sensors. Figures 21-25 show all winter minimums, while Figures 26-30 show the fifty coldest minimums at each sensor and Figures 31-35 show the fifty coldest NARR minimums.

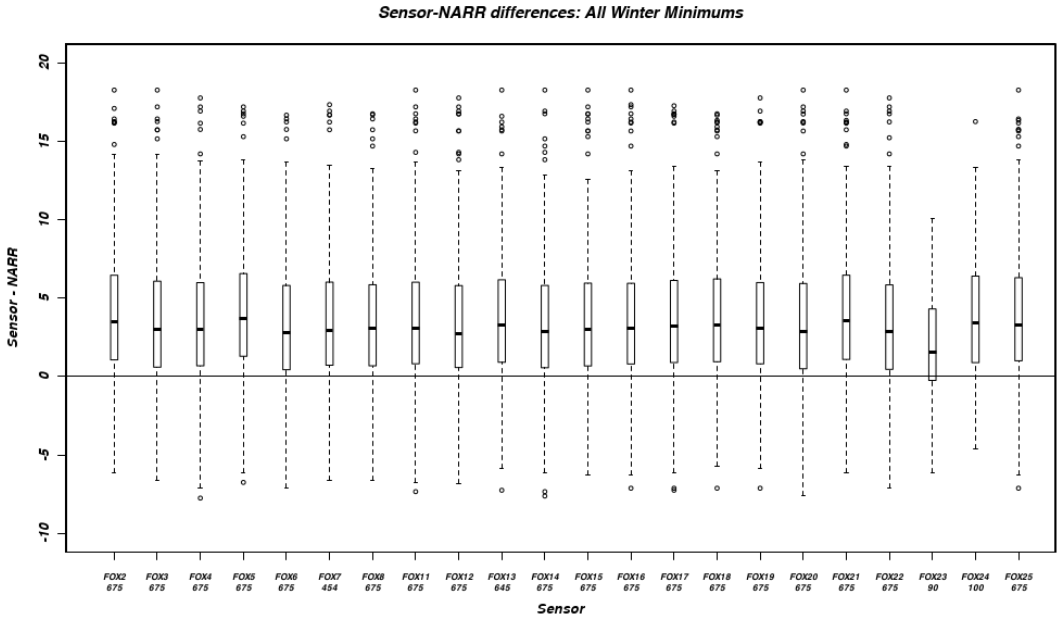

Figure 21- Sensor – NARR daily minimum temperature differences [ºC] on all nights in the study period for each Fox Run sensor. The number on the x-axis below each sensor name indicated the number of records represented by the boxplot on this and future figures.

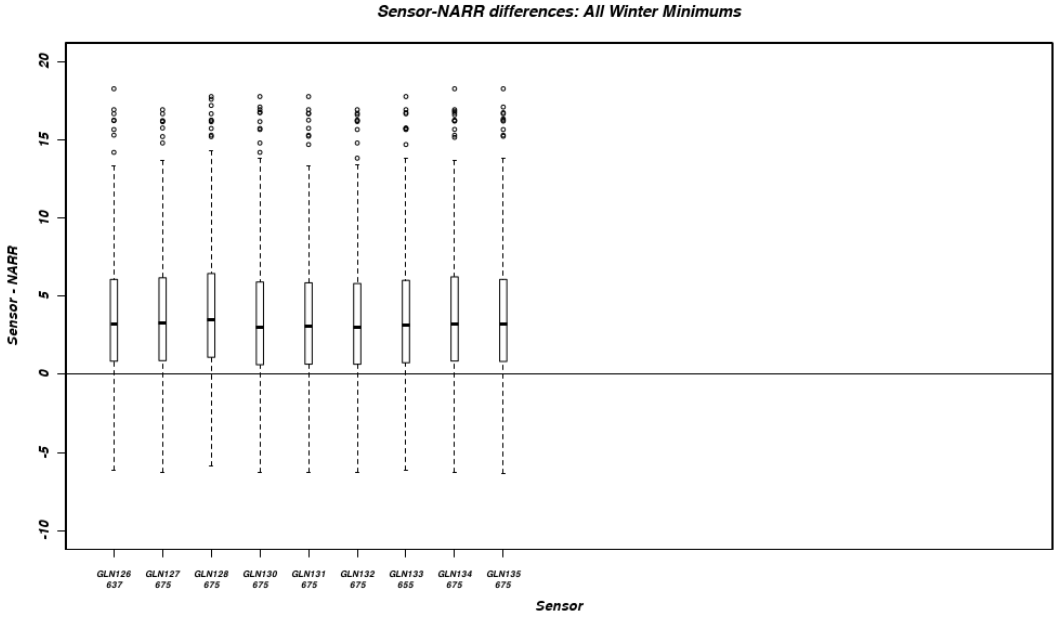

Figure 22- Sensor – NARR daily minimum temperature differences [ºC] on all nights in the study period for each Glenora sensor.

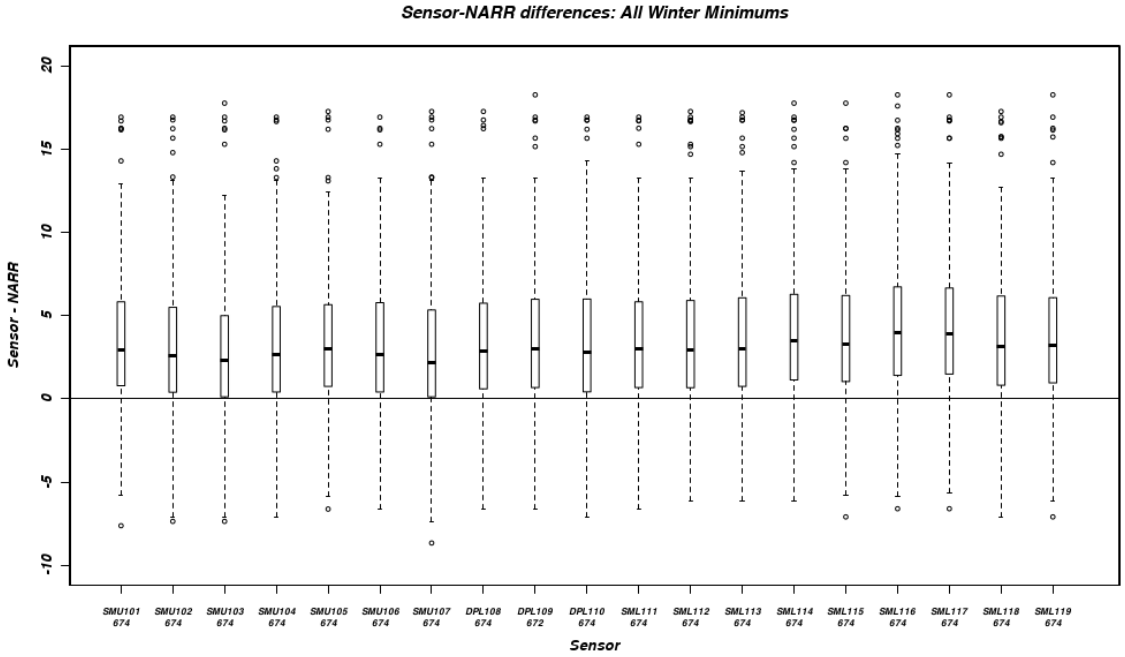

Figure 23- Sensor – NARR daily minimum temperature differences [ºC] on all nights in the study period for each Hazlitt sensor.

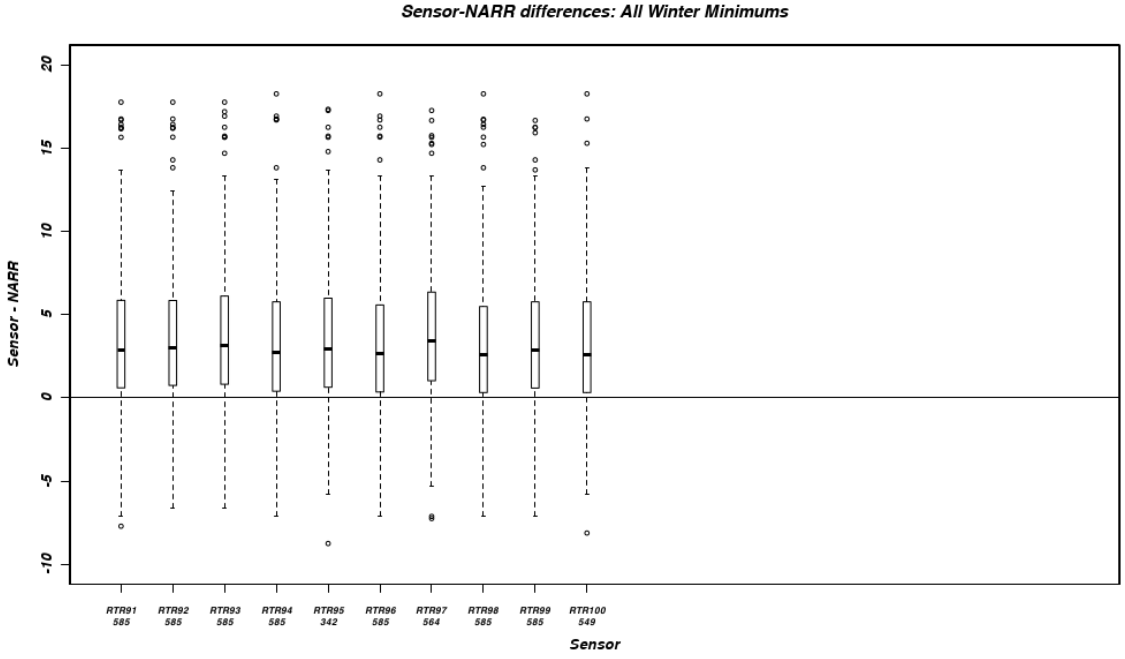

Figure 24- Sensor – NARR daily minimum temperature differences [ºC] on all nights in the study period for each Red Tail Ridge sensor.

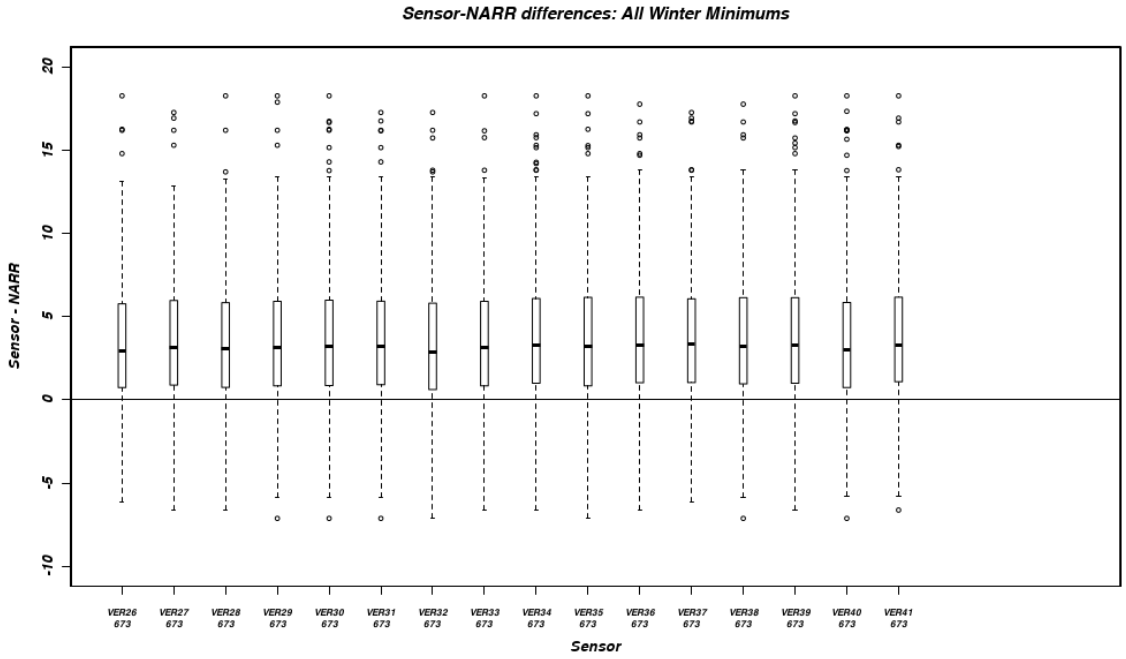

Figure 25- Sensor – NARR daily minimum temperature differences [ºC] on all nights in the study period for each Verill sensor.

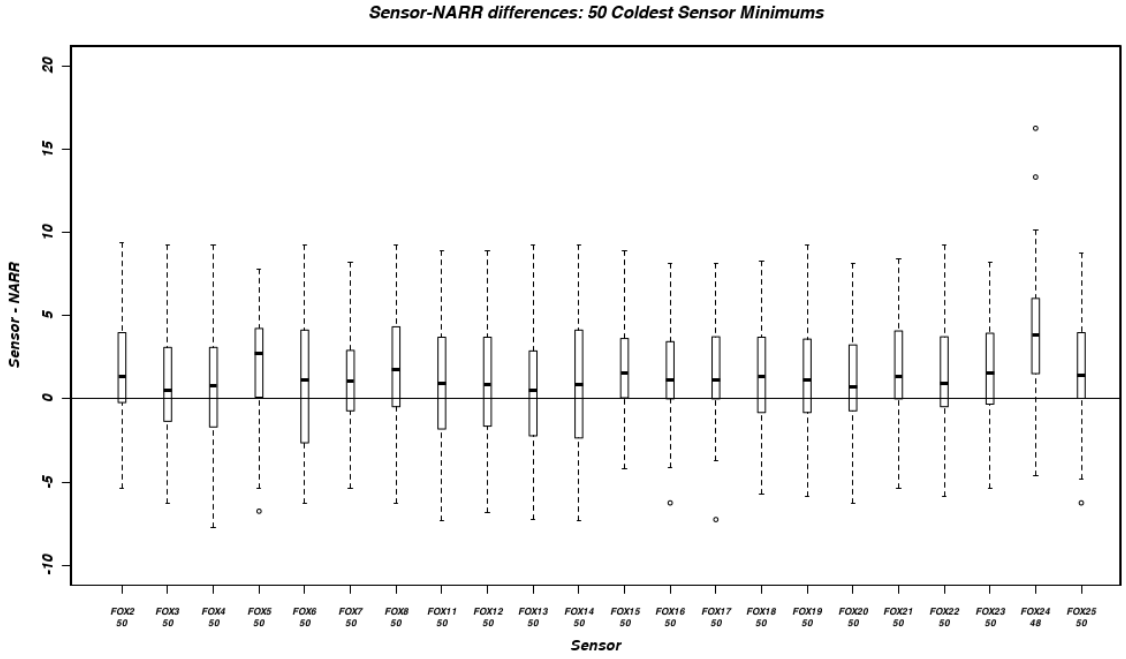

Figure 26- Sensor – NARR daily minimum temperature differences [ºC] for the 50 coldest daily minimums at each sensor during the study period at Fox Run.

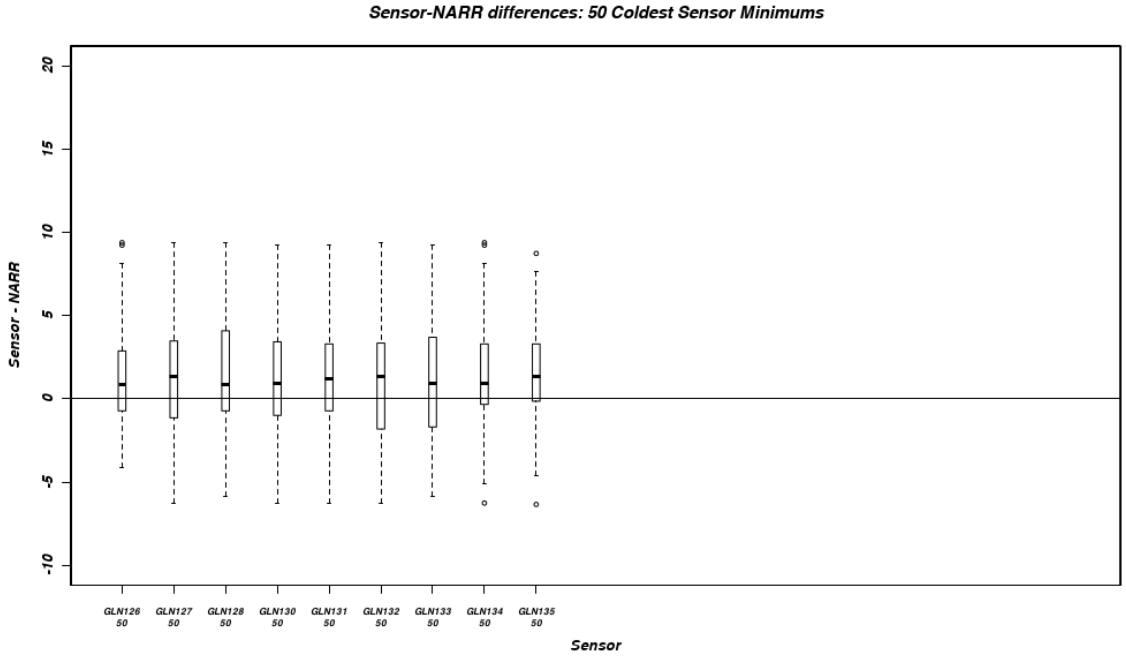

Figure 27- Sensor – NARR daily minimum temperature differences [ºC] for the 50 coldest daily minimums at each sensor during the study period at Glenora.

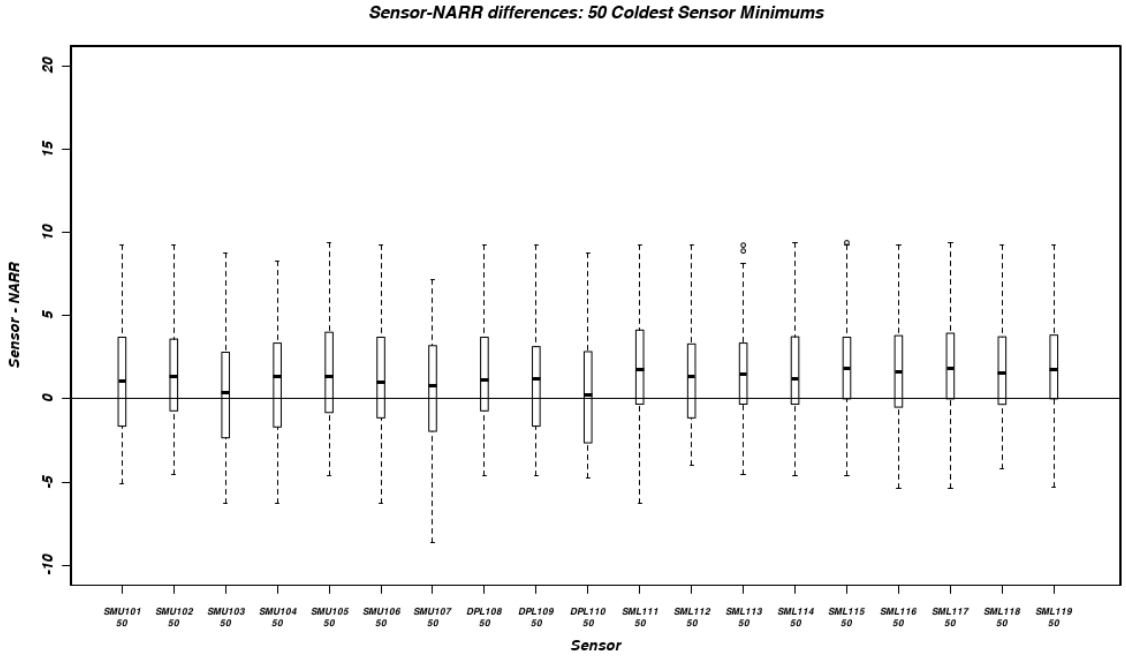

Figure 28- Sensor – NARR daily minimum temperature differences [ºC] for the 50 coldest daily minimums at each sensor during the study period at Hazlitt.

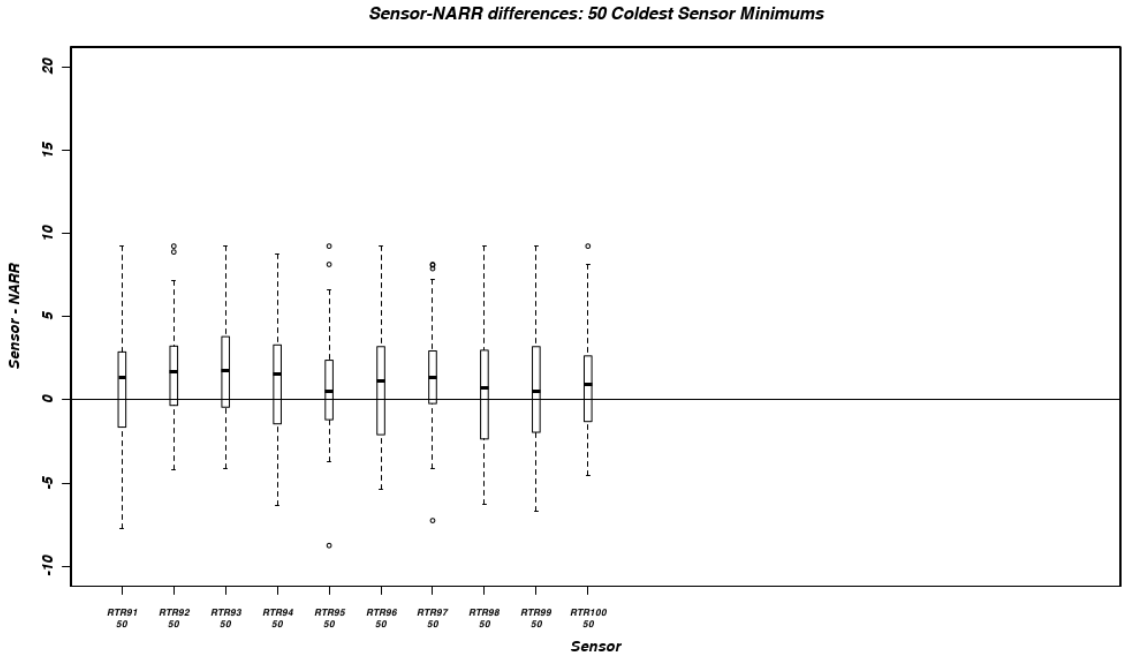

Figure 29- Sensor – NARR daily minimum temperature differences [ºC] for the 50 coldest daily minimums at each sensor during the study period at Red Tail Ridge.

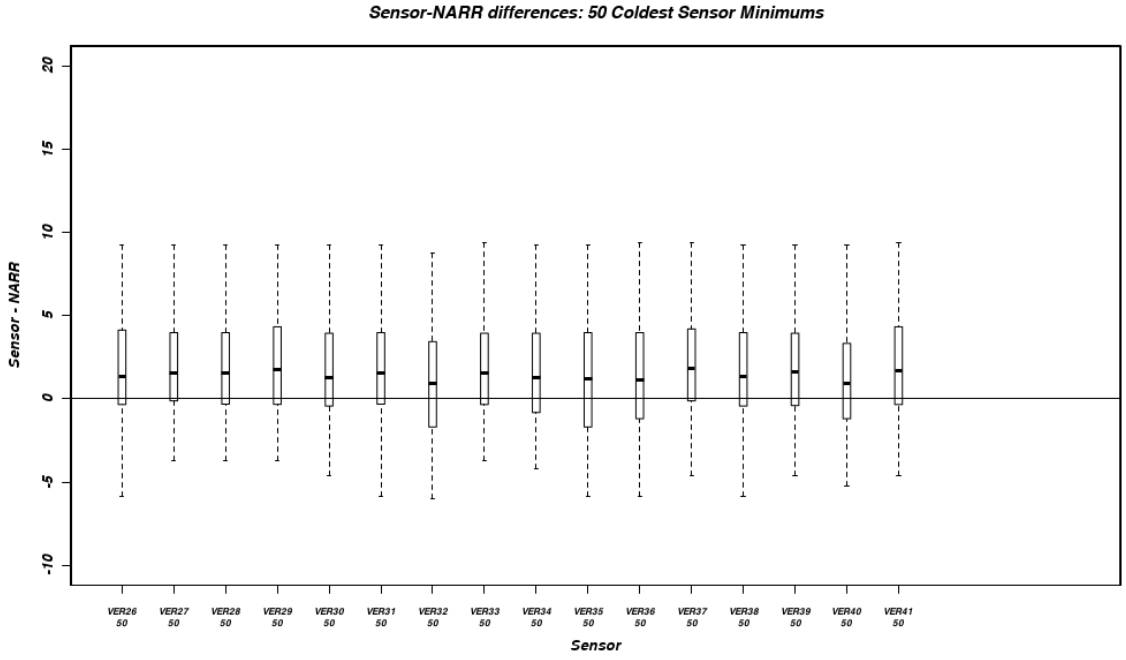

Figure 30- Sensor – NARR daily minimum temperature differences [ºC] for the 50 coldest daily minimums at each sensor during the study period at Verill.

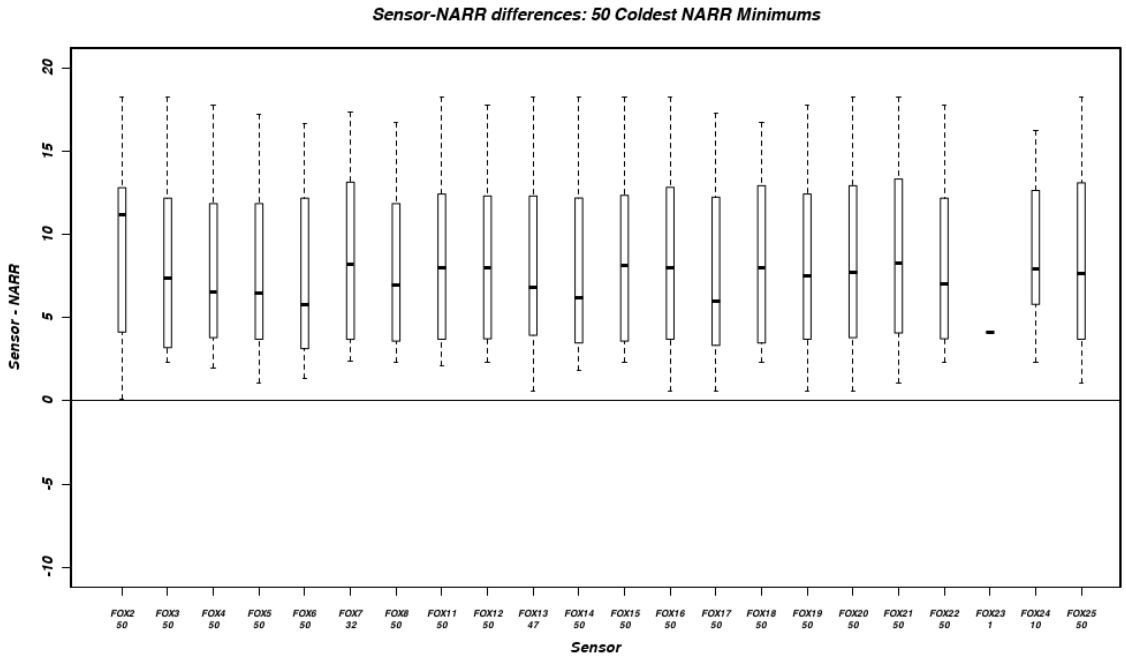

Figure 31- Sensor – NARR daily minimum temperature differences [ºC] for the 50 coldest daily minimums in the NARR data set during the study period for each Fox Run sensor.

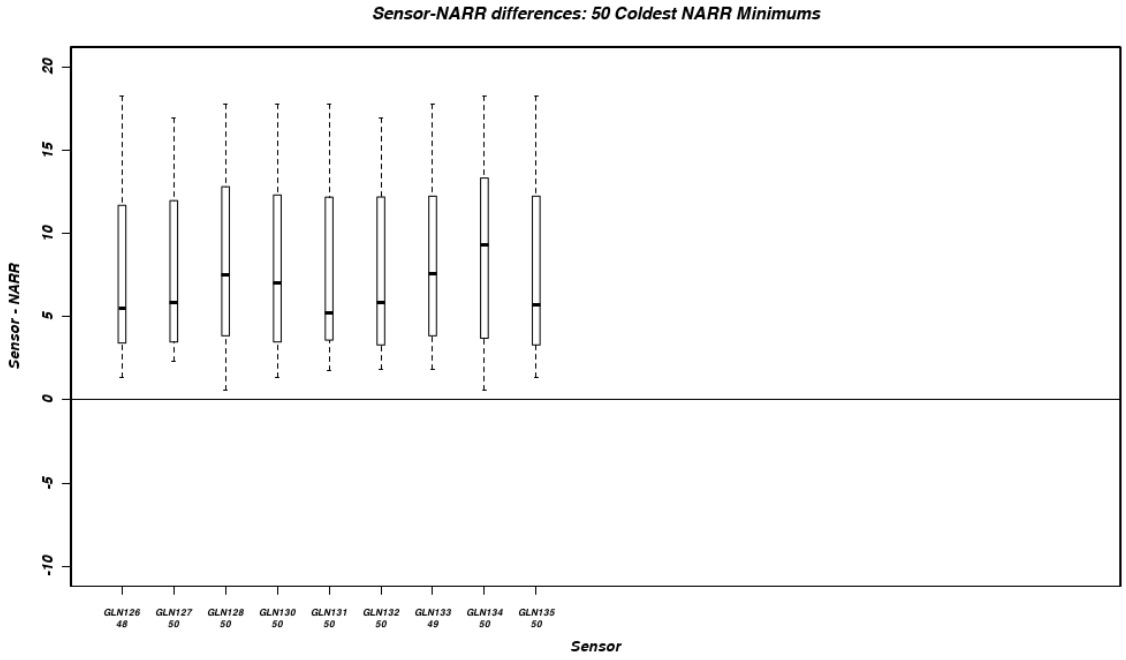

Figure 32- Sensor – NARR daily minimum temperature differences [ºC] for the 50 coldest daily minimums in the NARR data set during the study period for each Glenora sensor.

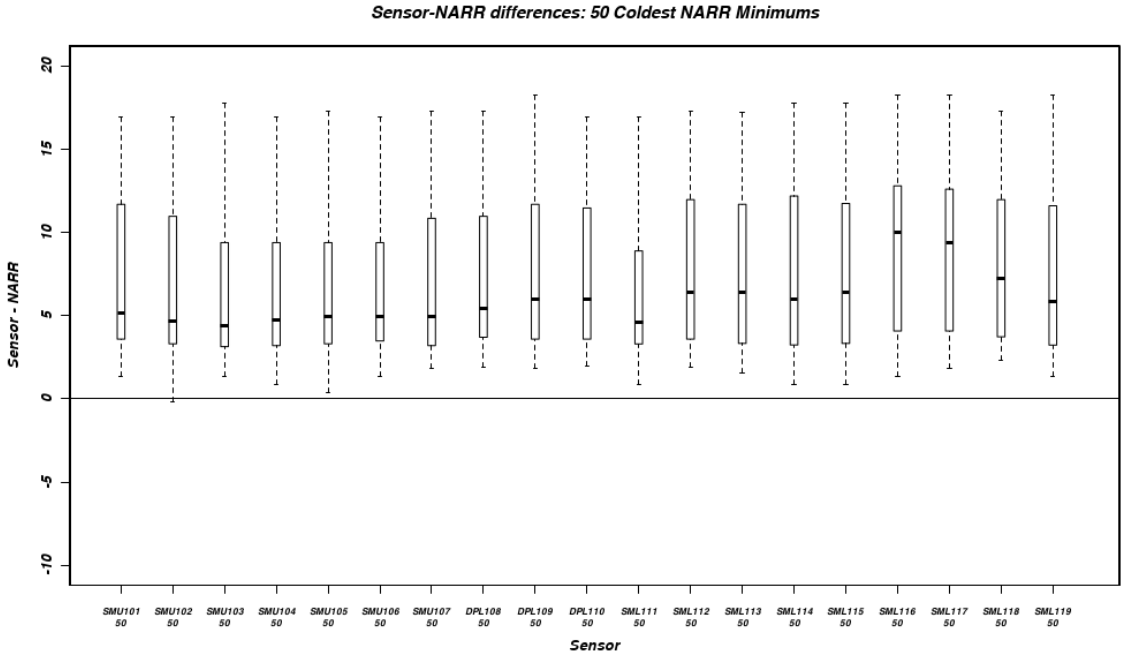

Figure 33- Sensor – NARR daily minimum temperature differences [ºC] for the 50 coldest daily minimums in the NARR data set during the study period for each Hazlitt sensor.

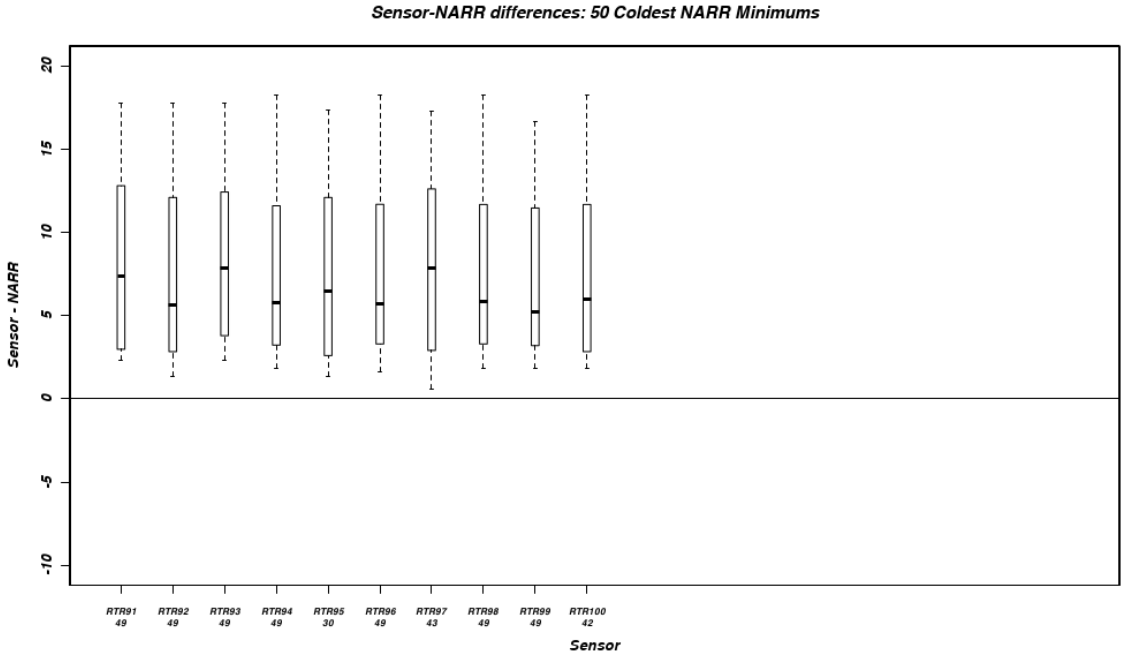

Figure 34- Sensor – NARR daily minimum temperature differences [ºC] for the 50 coldest daily minimums in the NARR data set during the study period for each Red Tail Ridge sensor.

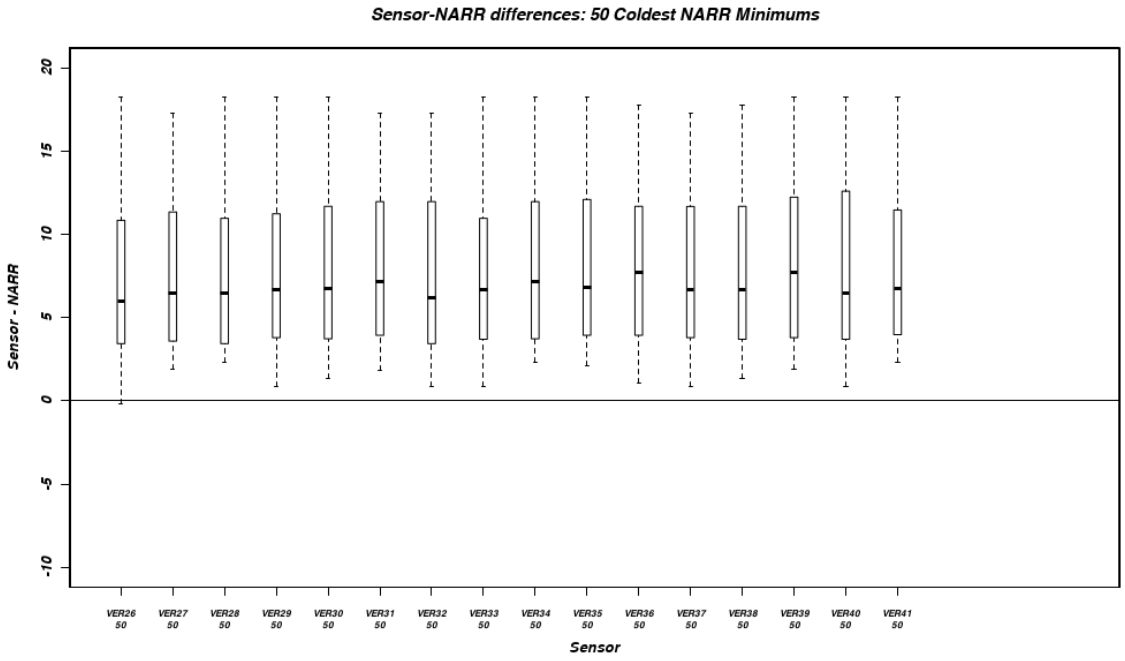

Figure 35- Sensor – NARR daily minimum temperature differences [ºC] for the 50 coldest daily minimums in the NARR data set during the study period for each Verill sensor.

When analyzing these 15 plots, a few observations become apparent. First the sensors typically measure warmer temperatures than does the NARR. This consistent bias very well may be attributed to the fact that the sensors are located in areas suitable for viticulture. Since viticulture is active in all sensor locations, it is not surprising that these locations are warmer than the ambient regional conditions.

Still, other features are apparent in the data. Sensors near the lake routinely measure warmer temperatures than sensors farther from the lake. This can especially be seen for sensors SML 116 and 117 on Figures 23, 28 and especially 33, where these two sensors have median temperatures of 9-10 degrees C greater than the NARR, compared to median temperatures of 5-7 degrees C greater than the NARR for

other Hazlitt sensor temperatures on the coldest NARR nights. This observation makes sense, given the relative warmness of Seneca Lake compared to the winter air.

Also worth noting is a general cool pattern associated with sensors just upslope from a tree line. This is most evident on Figure 29, the coldest sensor minimums at Red Tail Ridge. Sensor RTR 95 shows a median difference just above zero, while the upper quartiles are colder than the other sensors. It is also worth noting that the largest negative difference between a sensor's minimum and one of the 50 coldest NARR minima occurs at RTR 95. It can be assumed that cold air drainage is blocked by the presences of trees, leading to extra accumulation of cold air.

4) Testing Air Drainage Variables

To further investigate the observations made from the previous data plots, three individual sensors were selected based on their behavior in the previous data plots. SML 117 was chosen to represent sensor temperatures influenced by the lake, while RTR 95 was chosen as a tree line influenced sensor. VER29 was chosen as a control due to its proximity far from the lake, lack of nearby tree lines and for exhibiting no obvious trends in the previous analyses. The differences in minimum winter temperatures for these three sensors were plotted side by side for the fifty coldest sensor minimums.

As can be seen in Figure 36, the tendency for RTR 95 to have temperatures closer to the cold NARR temperatures is evident by having lower temperature values for all aspects of the box and whisker plot. It is interesting to note, however, that SML117 and VER 29 have very similar plots. This does not necessarily mean that SML117 and VER 29 have the same temperatures, only that on their coldest nights, they compare

similarly to the NARR. With the lake influencing SML 117 and a lack of mechanisms to pool cold air at VER29, it could be that the coldest nights at these two sensors are not always driven by radiational cooling.

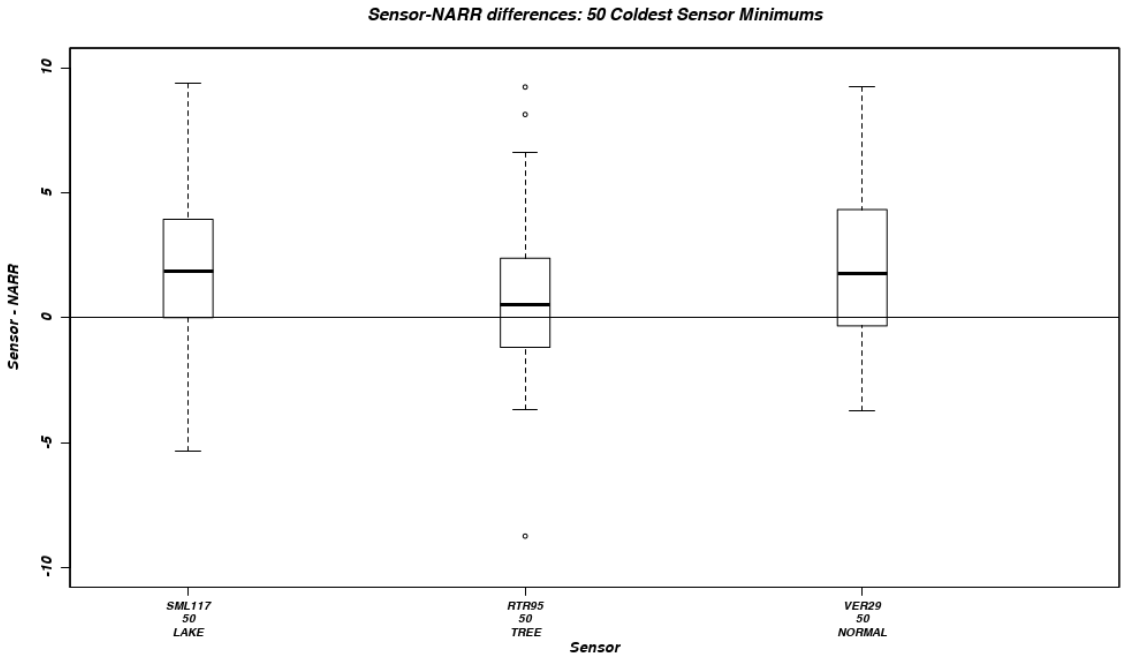

Figure 36- Sensor – NARR daily minimum temperature differences for the 50 coldest daily minimums at each of three sensors during the study period. The three sensors were selected to represent an influence from the lake (SML117), influence from tree lines (RTR 95) and no obvious influences (VER 29).

For each of the fifty lowest sensor minima, it was determined if the date on which the minimum occurred corresponded to one of the dates on which the NARR was at its lowest as well. Figure 37 shows interesting results from this analysis. First, there is a split between nights during which the sensor is within its fifty coldest, but the NARR is not and when both the sensor and NARR are at their coldest. When both the sensor and NARR are at their coldest, the NARR temperature is much lower than the sensor temperature. Conversely, when the sensor temperature is cold, but the NARR temperature is not, there is good agreement between the sensor and NARR. This result

can be attributed to the location bias. Since the sensor temperatures are, by nature of their location, warmer than the NARR temperatures, it would make sense to have sensor and NARR temperatures in better agreement when the sensor temperatures are at their coldest, but the NARR is not since the cold sensor effectively erases the preexisting bias.

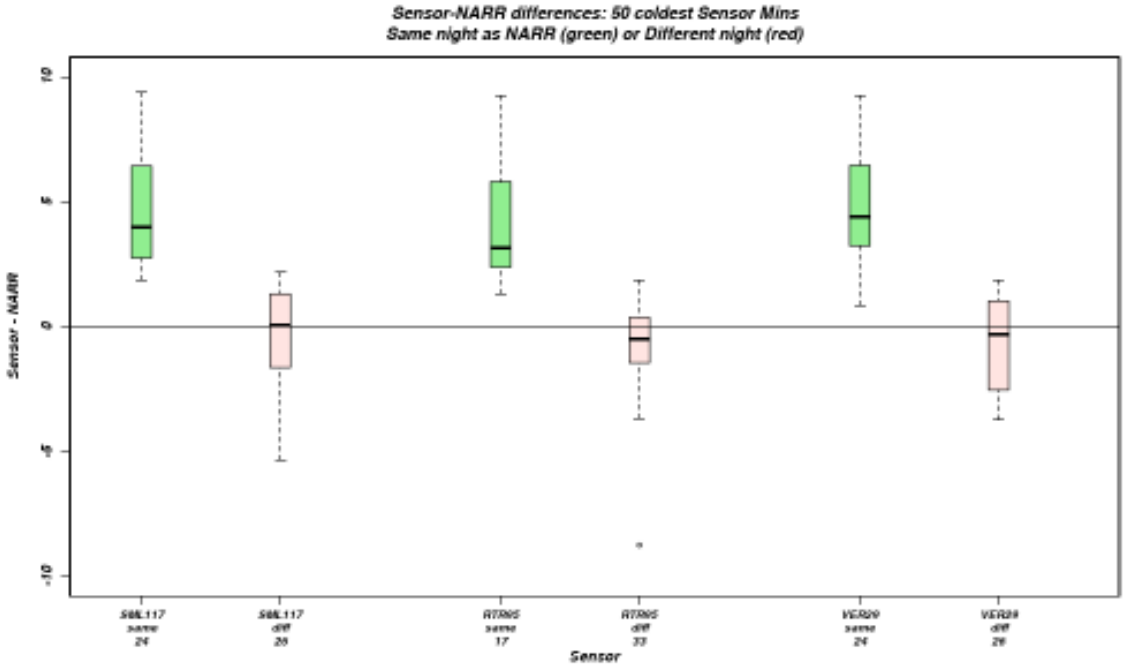

Figure 37- Sensor – NARR daily minimum temperature differences for the 50 coldest daily minimums at SML 117, RTR 95 and VER29 during the study period. Green plots represent coldest sensor minimums that occurred on nights that were also in the dataset of coldest NARR minimums, while pink plots represent those coldest minimums that occurred on nights not in the NARR dataset of coldest minimums.

Another observation to note is that the number of cases in each of the SML 117 and VER 29 plots are the same, while RTR 95 has many more cases when its coldest minimum is not in the NARR coldest minimum dataset. This further supports the hypothesis that the blockage of cold air drainage by the tree line downslope of RTR 95 may have a major impact on cooling the air just upslope.

It was assumed that cold air drainage would dominate under conditions conducive to radiational cooling. Three variables characteristic of radiation cooling were evaluated to see if these conditions could be determined based on these variables. The fifty coldest sensor minimums were compared to the NARR minimums on the corresponding date. Cloud cover, 10m wind speed and the 2-30m lapse rate at 1200 UTC were also obtained from the NARR on these days and used to stratify the differences between the sensor and NARR minimums.

The results of cloud cover plot, shown in Figure 38, were difficult to interpret. For example, RTR95, shown in green, seemed to be coldest under mixed sky conditions, while clear and cloudy skies yielded similar results. A similar pattern can also be seen in SML 117 and VER 29. The 10m wind speed plot, Figure 39, also yielded inconsistent results, with generally little variation in the medians of the box plots. The 2-30m lapse rates in Figure 40 however did show a clear pattern of sensor-NARR difference that were related to the presence of an inversion. Lapse rates trend from negative to increasingly positive from left to right on the plot, with positive lapse rates signifying an inversion. A general upward trend can be seen in the median differences when looking from negative to positive. However, lack of data is a problem in most of these plots. Generally fewer than 5 data points comprise each box plot. The 2-30m lapse rate was further analyzed with more data to further investigate this observed trend.

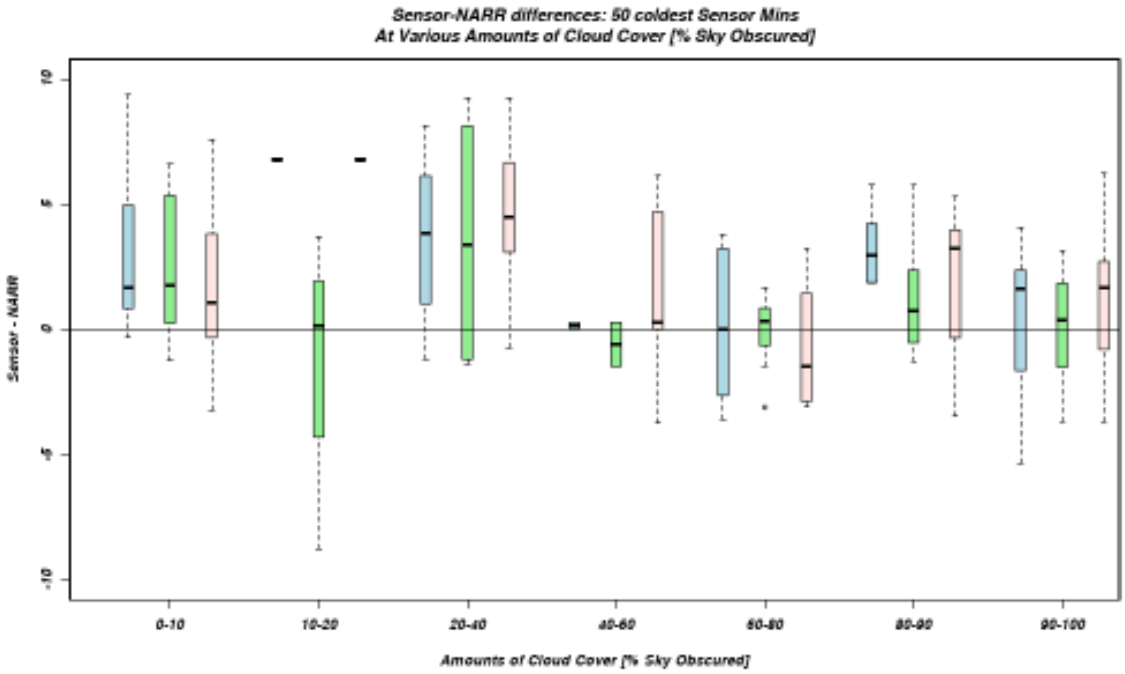

Figure 38- Sensor – NARR daily minimum temperature differences for the 50 coldest daily minimums at SML 117 (blue), RTR 95 (green) and VER29 (pink) during the study period. Each set of three plots represents the amount of cloud cover that occurred at 12 UTC on the day of that minimum, as determined from the NARR data set.

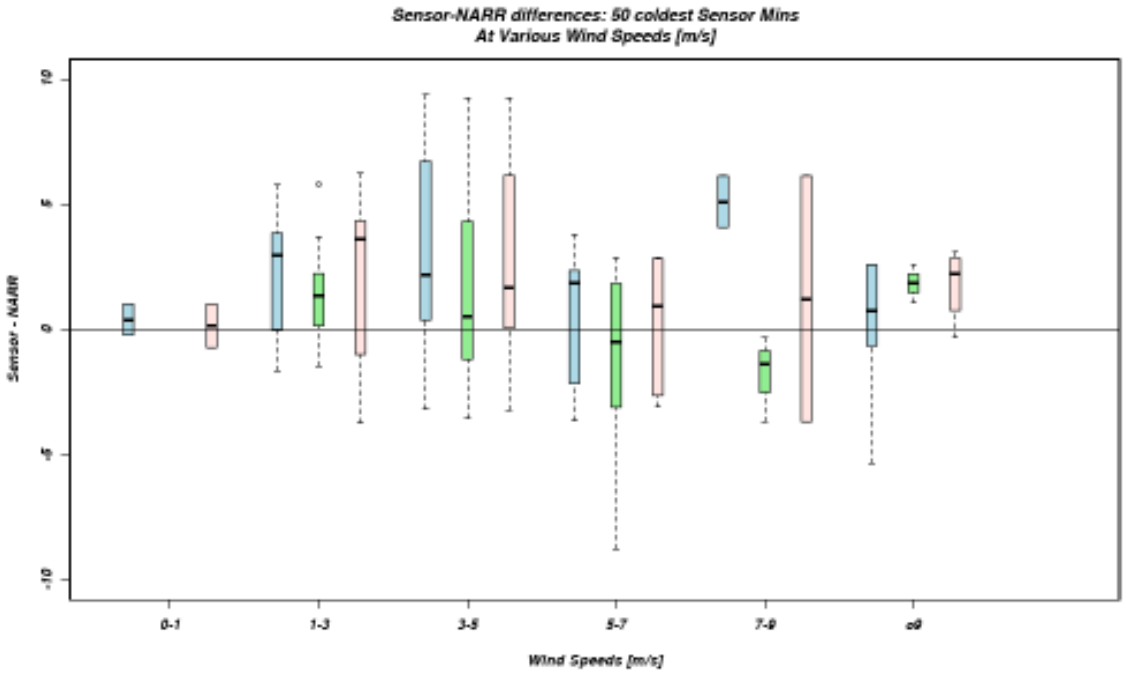

Figure 39 Sensor – NARR daily minimum temperature differences for the 50 coldest daily minimums at SML 117 (blue), RTR 95 (green) and VER29 (pink) during the study period. Each set of three plots represents the 10m wind speed that occurred at 12z on the day of that minimum, as determined from the NARR data set.

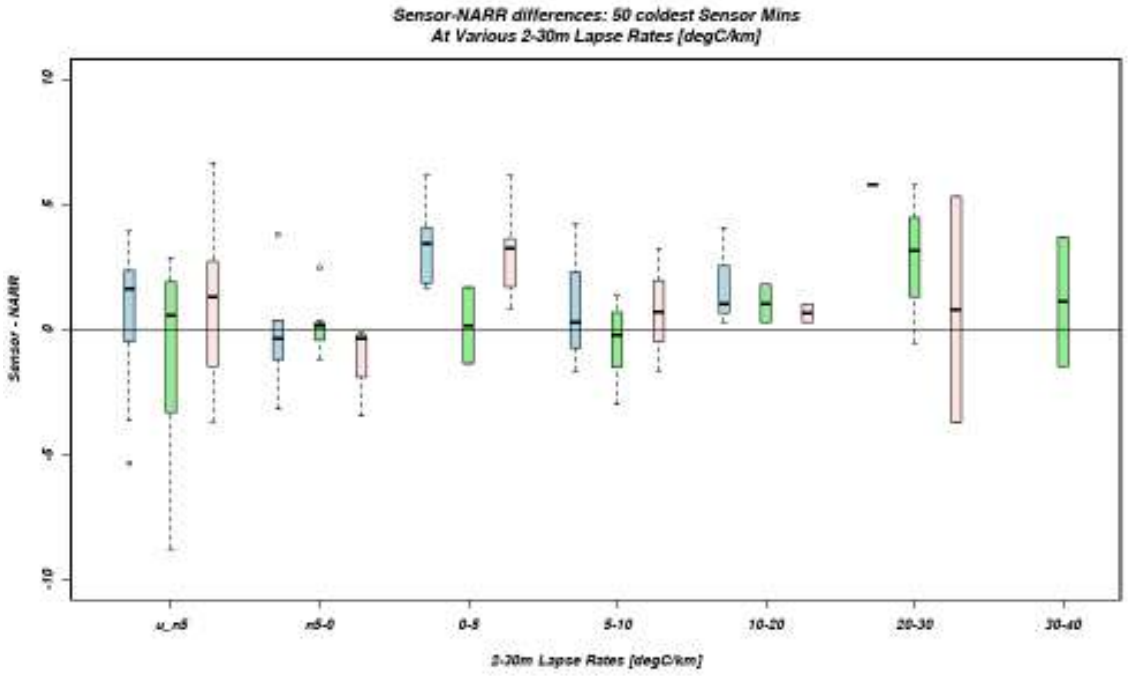

Figure 40- Sensor – NARR daily minimum temperature differences for the 50 coldest daily minimums at SML 117 (blue), RTR 95 (green) and VER29 (pink) during the study period. Each set of three plots represents the 2-30m lapse rate that occurred at 12z on the day of that minimum, as determined from the NARR data set.

5) 2-30m Lapse Rate Analyses

Two steps were taken to increase the number of data points in each box plot. First, the lapse rate was dis-aggregated down into three categories instead of the seven previously used. All non-inversions were grouped together as one set, while weak inversions with lapse rates less than 15 degrees C/km were another set. The third and final set was for strong inversions having lapse rates over 15 degrees C/km. The strong lapse rates may seem extreme at first, but it is important to remember that these lapse rates are confined to the lowest 28m of the boundary layer.

Secondly, all 74 sensors were classified into one of 5 categories: those very near the lake, those farther from the lake, but still within its influence, those just outside of the

influence of the lake, sensors with possible tree line influence and then all other sensors, which were called ‘normal’. Lake sensor classification was determined from the NRCC lake influence study. Sensors with a Lake Index less than 8,000 m^2 were considered near the lake, those with a Lake Index between 8,000 m^2 and 25,000 m^2 considered farther from the lake, and those with a Lake Index between 25,000 m^2 and 45,000 m^2 being placed in the ‘outside’ category. Preference was given to tree line sensors over all other categories since most of the sensors identified as tree line sensors could also be placed in one of the three lake categories.

The differences between the minimum temperatures of the sensor and the NARR on the fifty coldest nights of each sensor were again calculated. Each difference was then classified by its corresponding 1200 UTC NARR 2-30m lapse rate and the aforementioned sensor classification. The results of this analysis are show in Figure 41. An obvious upward trend in greater differences is seen as the lapse rate becomes more positive. This confirms the trend seen in Figure 40.

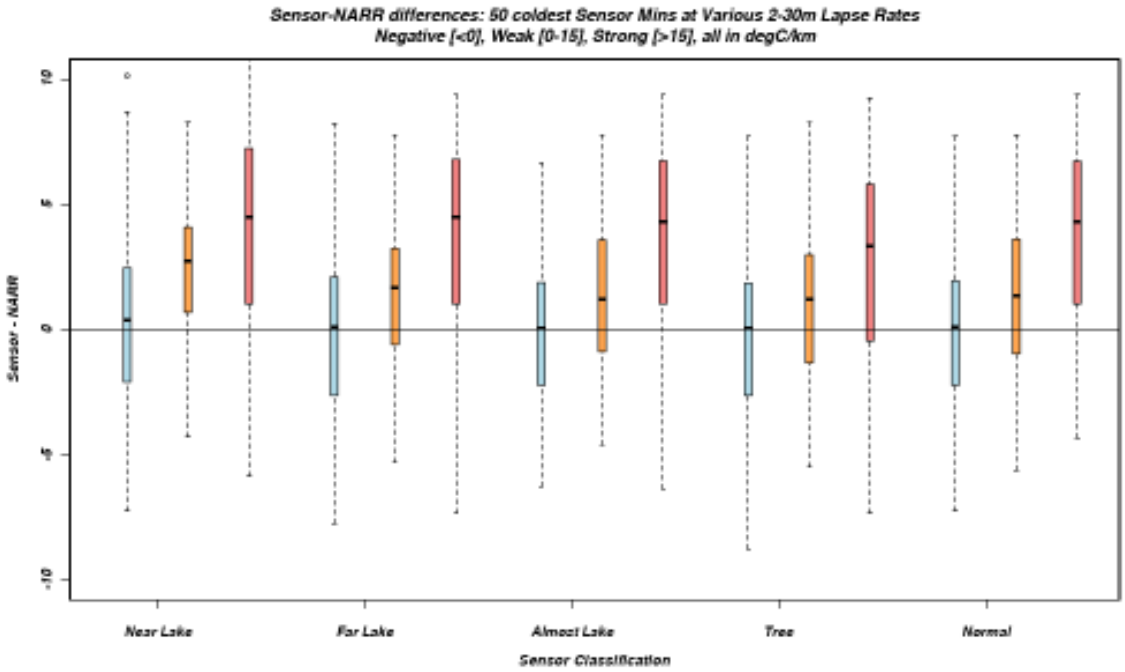

Figure 41- Sensor – NARR daily minimum temperature differences for the 50 coldest daily minimums at each sensor during the study period. Sensors are classified by location as having a high lake influence, low lake influence, just outside of the lake influence, tree influence, or no obvious influence. Each color of plots represents a different classification of the 2-30m lapse rate that occurred at 12z on the day of that minimum, as deteremined from the NARR data set, with blue representing non-inversions (<0 degC/km), orange representing weak inversion (0 to 15 degC/km) and red representing strong inversions (>15 degC/km).

A few other key observations are seen in Figure 41 as well. Sensors classified as having a tree influence showed much lower median differences than any other type of sensor under the strongest lapse rates. There is also a very slight, but still present, downward trend in medians at the strongest lapse rates going from sensors well within the lake's influence, to farther from the lake and finally outside of the lake's influence. Sensors that were just outside of the lake's influence also closely resembled the normal sensors, where no distinguishing characteristics were observed. Furthermore, all sensors compared very well with the NARR under non-inversion conditions. All of these observations seem to support the aforementioned hypotheses on tree and lake influences and maximum radiational cooling processes.

Figures 42 and 43 show the same analysis conducted with slight adjustments. Figure 42 shows the minimum temperature differences between the sensors and the NARR at the fifty coldest NARR minimums, while Figure 43 shows the comparison of all winter minimums. The same basic trends found in Figure 41 can also be seen in Figures 42 and 43, further strengthening the hypotheses.

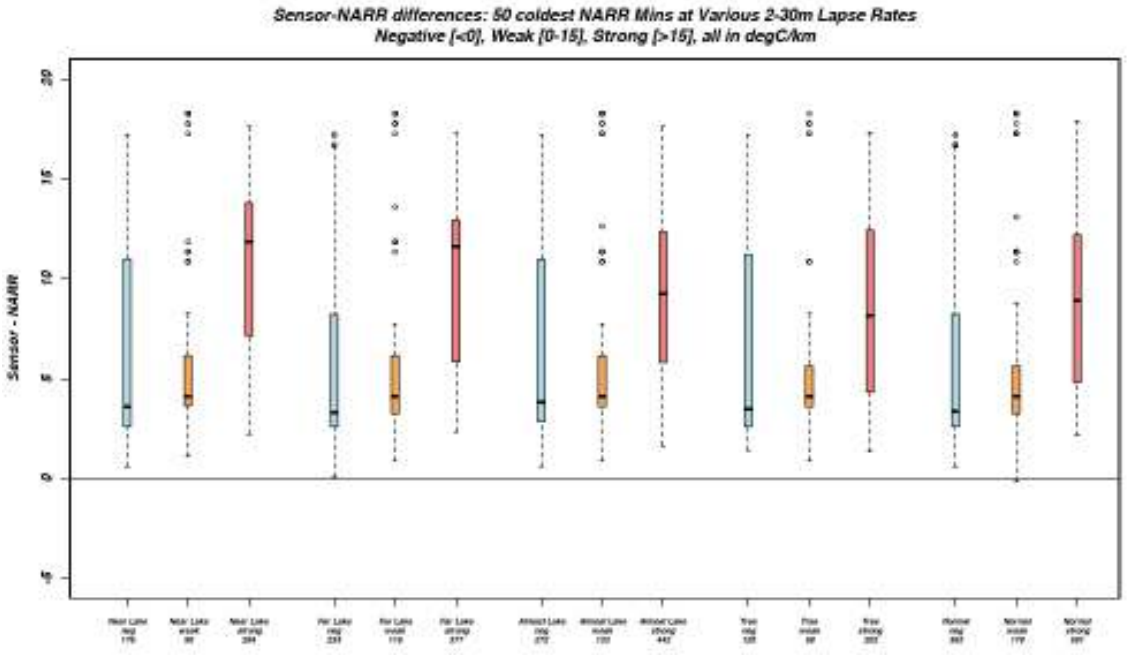

Figure 42- Same as Figure 41, but for sensor-NARR differences associated with the 50 coldest daily minimums in NARR dataset during the study period.

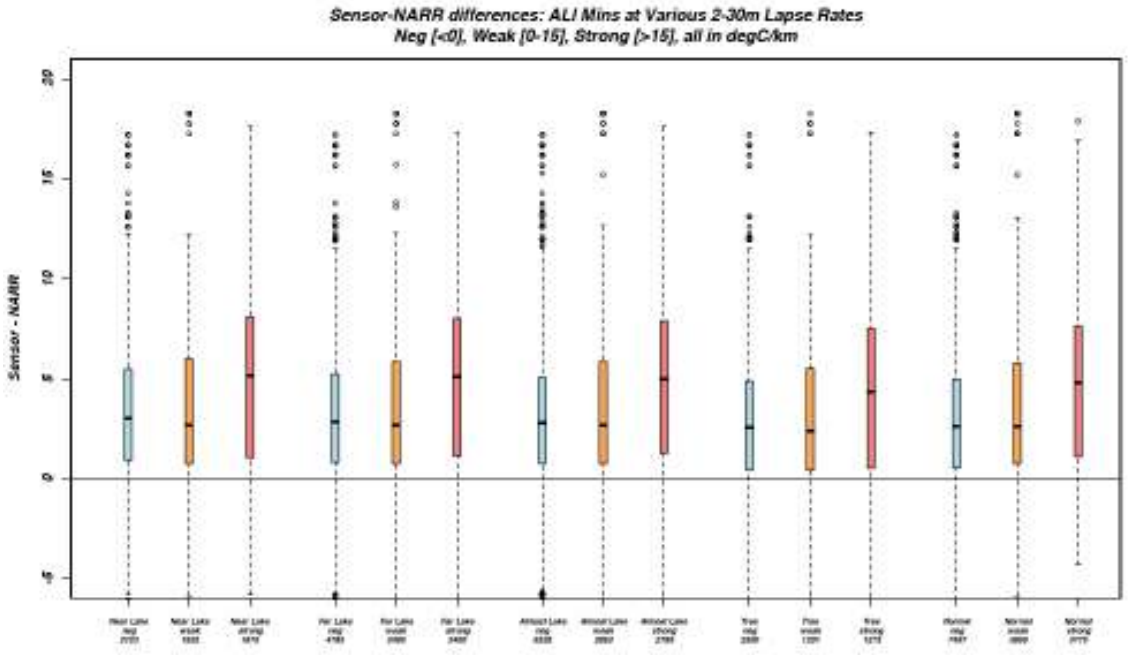

Figure 43- Same as Figure 40, but for sensor-NARR differences far all daily minimums in the study period.

6) Climatology

To compile a climatological record of temperatures over the Finger Lakes AVA, data were obtained from the NARR dataset for the seven grid cells that cover Seneca, Cayuga and Keuka lakes, along with an eighth cell that covers Owasco Lake (Figure 44). Temperature, pressure and height values were compiled for each grid at 0600 UTC, 0900 UTC and 1200 UTC for all nights in January, February, March and December from 1979-2011, a period of 32 years.

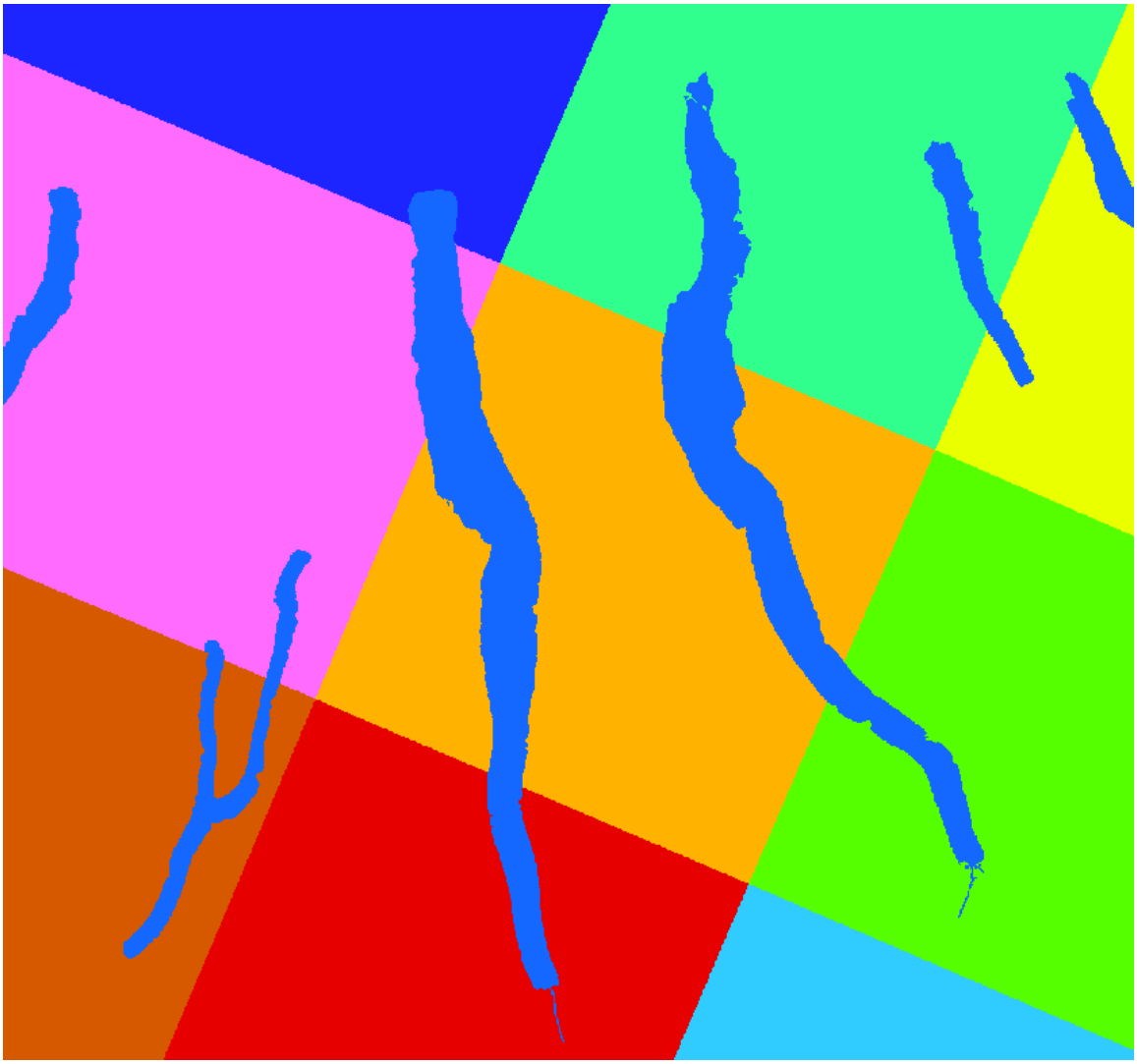

Figure 44- Spatial representation of the NARR dataset grid cells in the Finger Lakes Region.

Using ArcMap and a 10m digital elevation model (DEM) of the Finger Lakes region, a grid was created with the value of the lake influence, ranging from 0 to 40,000 m^2 as described in the previous section. For Cayuga and Keuka lakes, a ratio was established between the average width of Seneca Lake and the average width of each lake to calculate the maximum lake influence value of the individual lakes. Cayuga was found to have a maximum value of 33,759 m^2, while Keuka's influence was computed to be 15,104 m^2 (Figure 45).

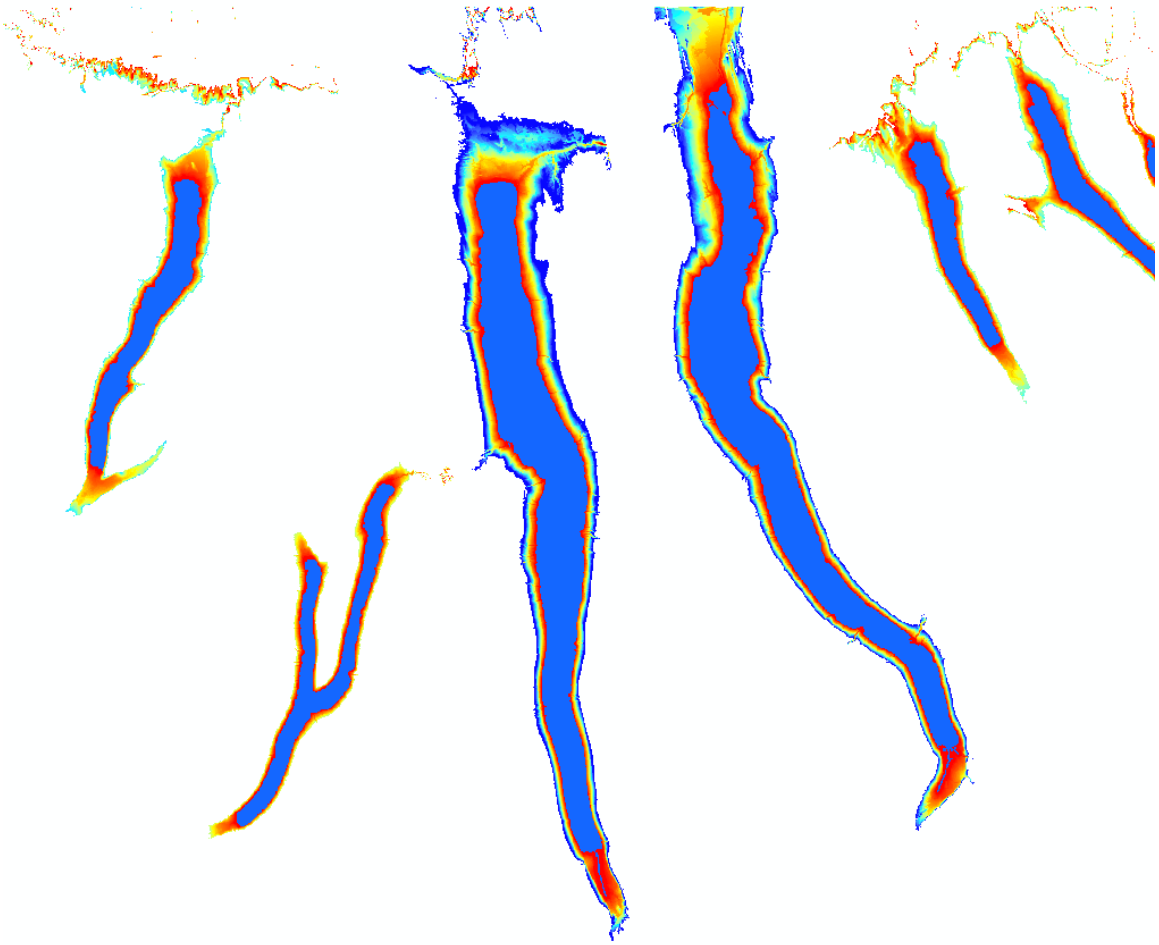

Figure 45- Map of areas of lake influence relative to each Finger Lake. Shading goes from high influence (red) to little influence (dark blue) on Seneca and Cayuga Lakes, with influence ending at the yellow shading on Keuka Lake. The lakes do not influence areas in white.

Temperatures at each grid point within the area of lake influence were then calculated for each hourly time period using the methods of lake adjustment described previously. Temperatures outside of the lake influence area were adjusted for location elevation differences from the NARR based on the 2-30m lapse rate (see Figure 40). Once the temperatures for each hour in the 32-year time period were calculated for all locations, both influenced and not influenced by the lakes, the daily minimum temperature for each location was calculated to serve as the basis for the climatology.

Grape vine injury is most prevalent at temperatures below -20° C and -24°C (Lakso, personal communication) for Vitis vinifera, the classic European wine grape. Locations that did not record minimum temperatures below -20°C during the 32 year period would have little winter freeze damage, no matter what variety of grape was grown (Figure 46). On the other hand, areas which experience temperatures of -24°C may experience damage to all but the hardiest native varieties of wine grapes (Figure 47). The number of times each of these thresholds was met over the 32-year period was calculated for each location. The calculated frequency values were then applied to the previously mentioned 10m-lake influence grid to display the data visually.

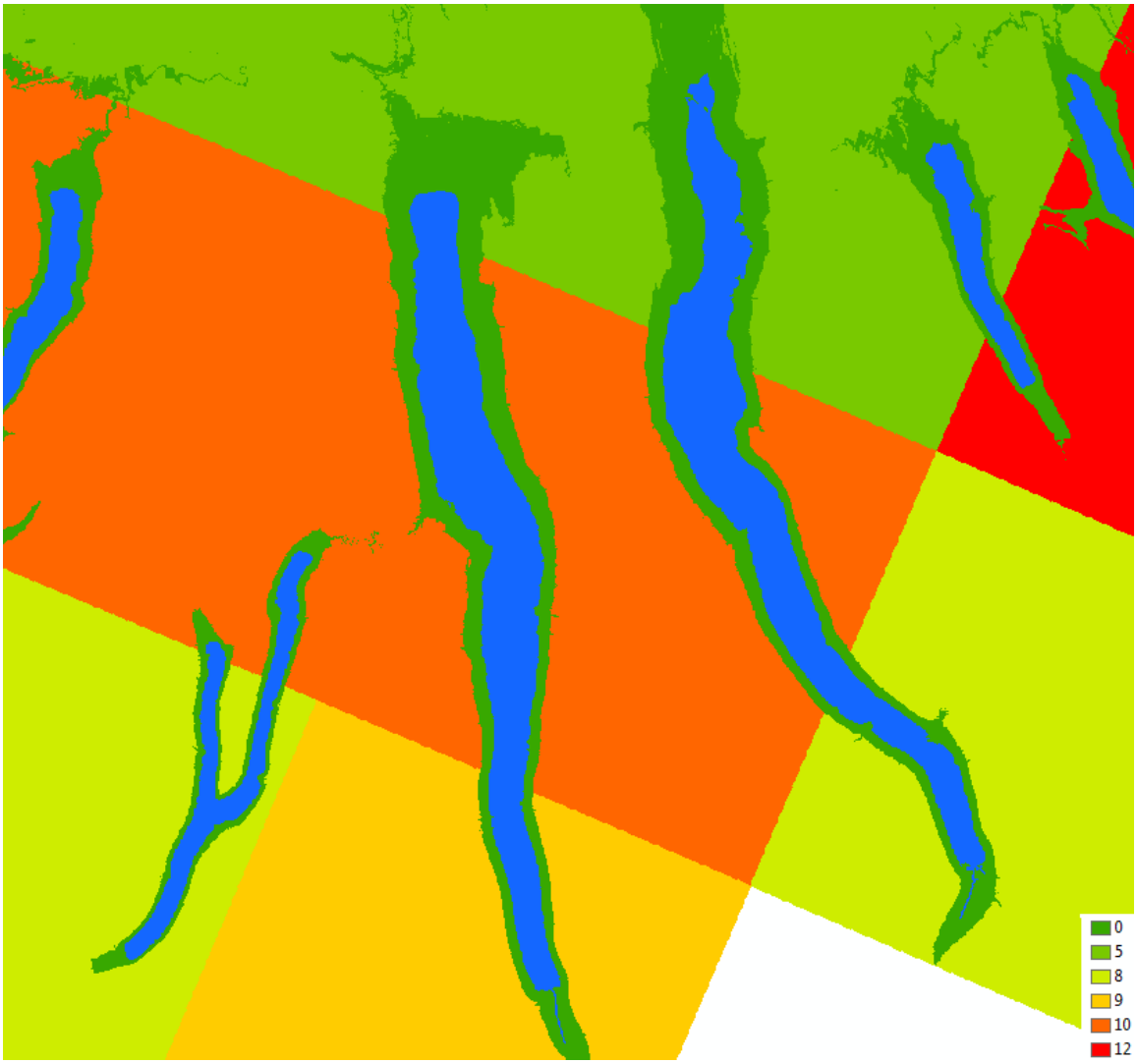

Figure 46- Number of occurrences of daily minimum temperatures below -20°C during the 32 year climatology period of 1979-2011.

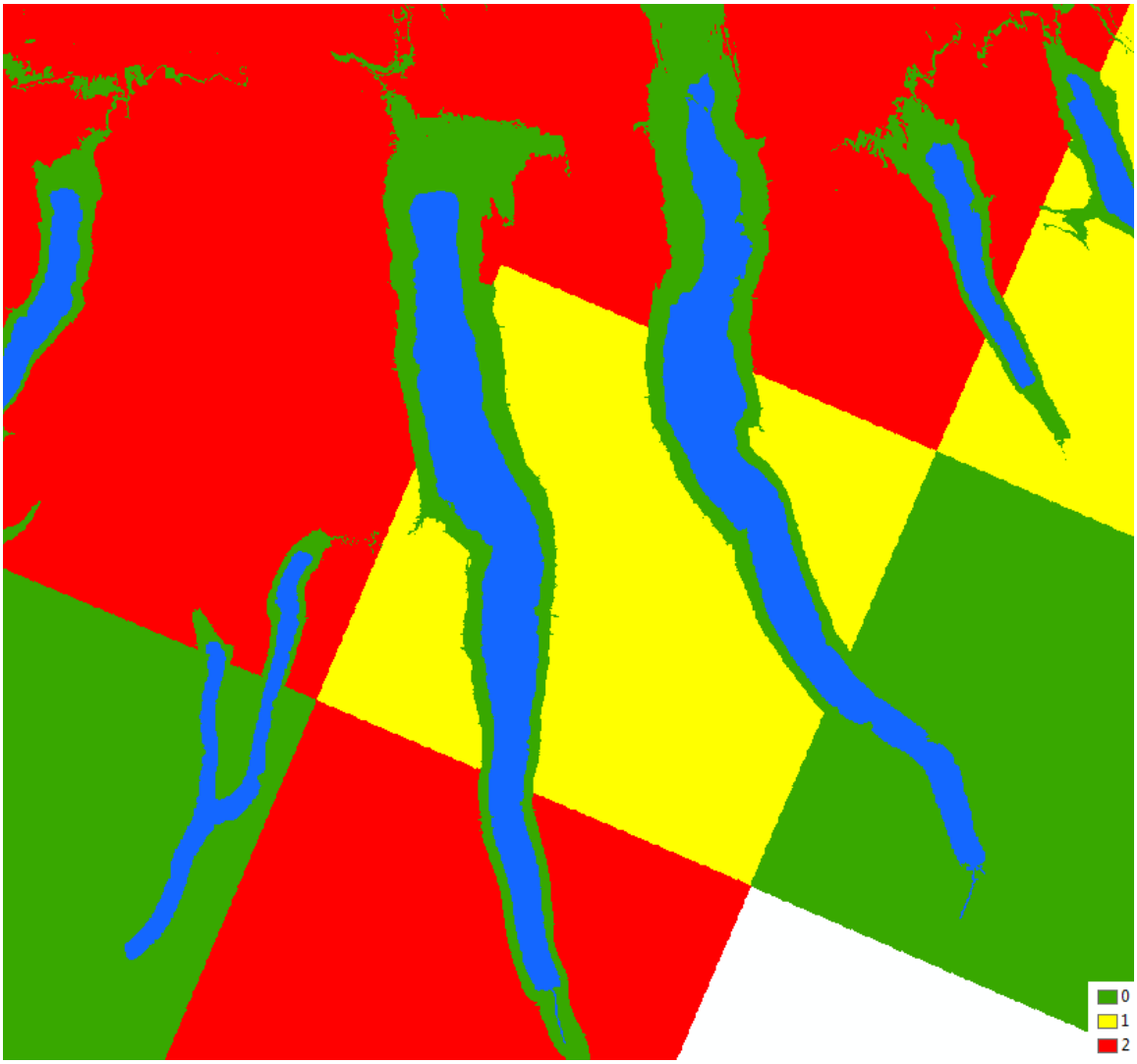

Figure 47- Number of occurrences of daily minimum temperatures below -24°C during the 32 year climatology period of 1979-2011.

The resulting two maps were then compiled together to give each value a single rating for its viticulture suitability with respect to the climatological minimum temperatures. Locations that recorded minimum temperatures colder than -24° C were coded with a 0, while locations that never recoded temperatures colder than -20° C were coded with a 2. All other locations were coded with a 1. These values can be interpreted as a 0-2 scale, ranging from unfavorable to favorable. All areas that were classified as within a given lake's influence resulted in a favorable classification, with

unfavorable and somewhat favorable classifications for areas outside of the influence of the lakes (Figure 48).

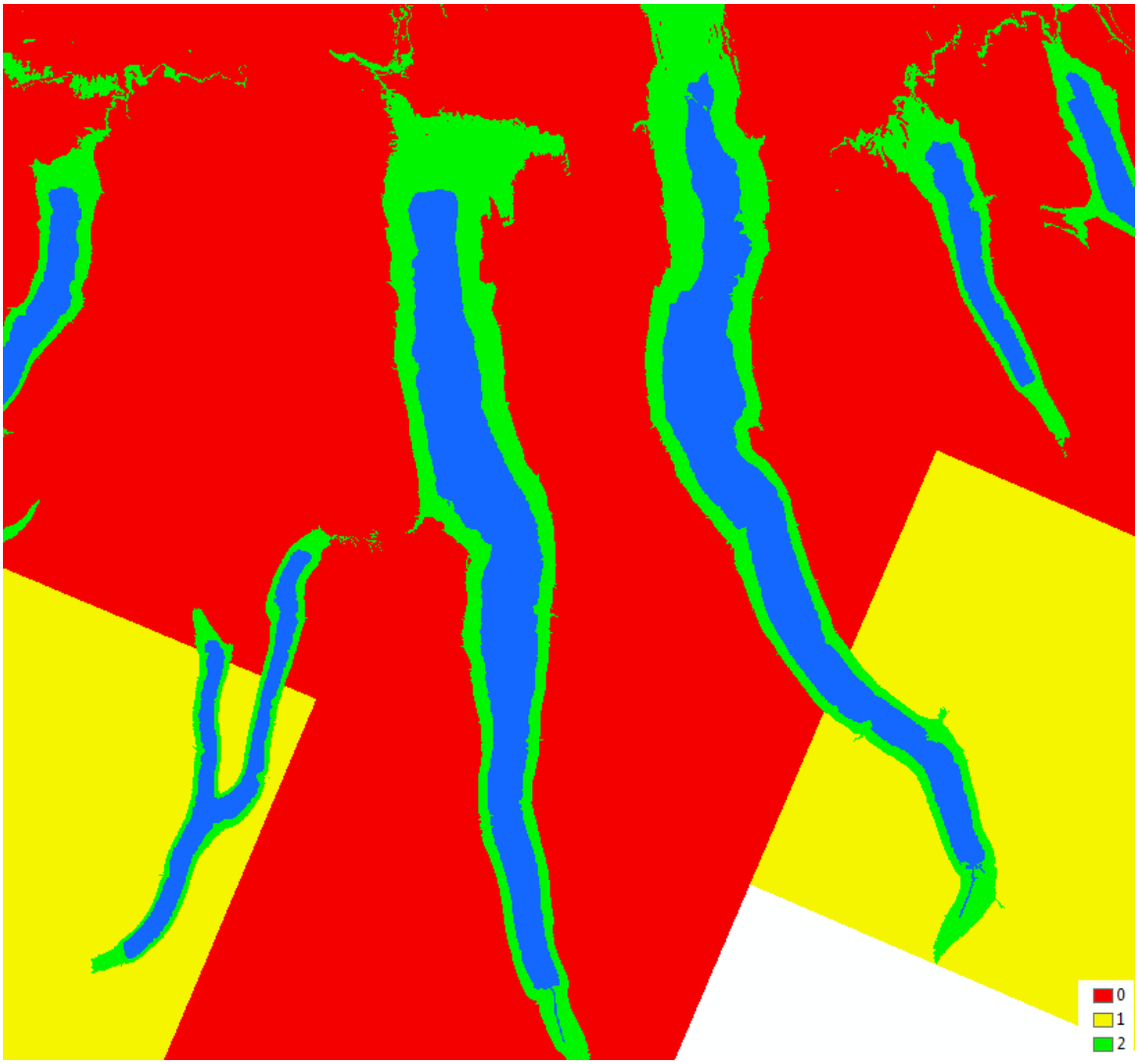

Figure 48- Temperature classifications of the Finger Lakes. Red areas are considered least suitable for viticulture, while green areas are most suitable.

Additionally, the presence of cold air flowing down the hillslope in channels, as was discussed in the exploratory analysis section, was modeled from the 10m-DEM. Using a built-in tool within the ArcMap GIS program, the 'flow direction' of each 10m cell was calculated. This tool works by comparing the elevation of a given cell to its eight surrounding neighbors and coding the direction of the highest drop in elevation. From

the results of this calculation, the number of cells at ‘flow’ to a single point can be calculated. This can then be used as a simulation for the flow of cold air down a hillslope, as was done in Chung et. al. (2006). Similar to Chung et. al., to calculate the accumulation of cold air with respect to how it influences the temperature at a given point, the flow accumulation was restricted to within 5 cells of the point, resulting in an 11 x 11 grid of 10m cells. This analysis was conducted for all locations within 2km of the shore of each lake. For areas farther away from the lake, the grid cell size was resampled to 100m, with the accumulation again being restricted to within 5 cells to all sides, resulting in an 11 x 11 grid of 100m cells. This approach was taken to drastically reduce the processing time of this intensive analysis (Figures 49 & 50).

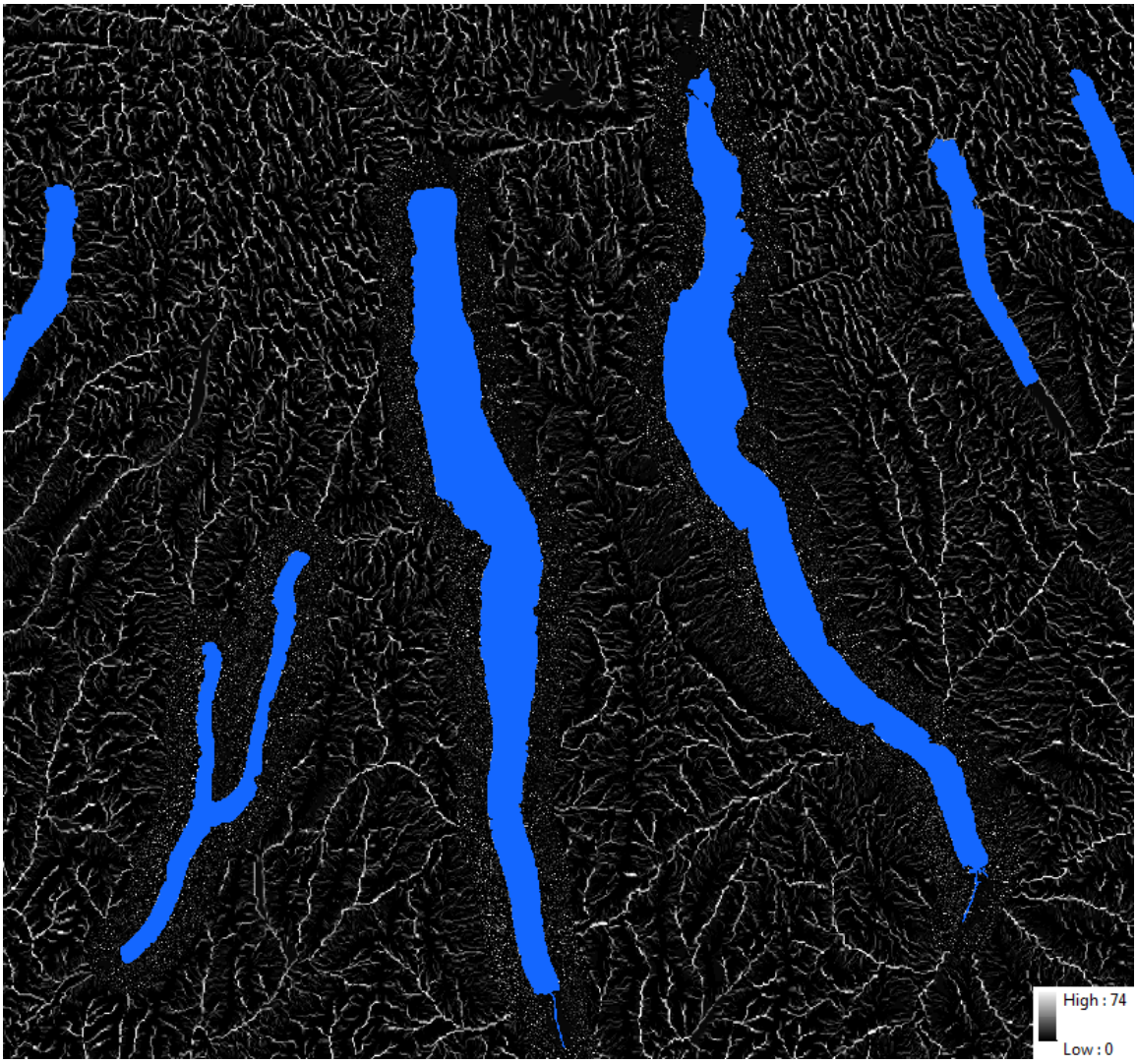

Figure 49- Modeled accumulation of cold air in the Finger Lakes. White areas have a higher concentration of cold air from downslope flow, while black areas have little to no cold air accumulation.

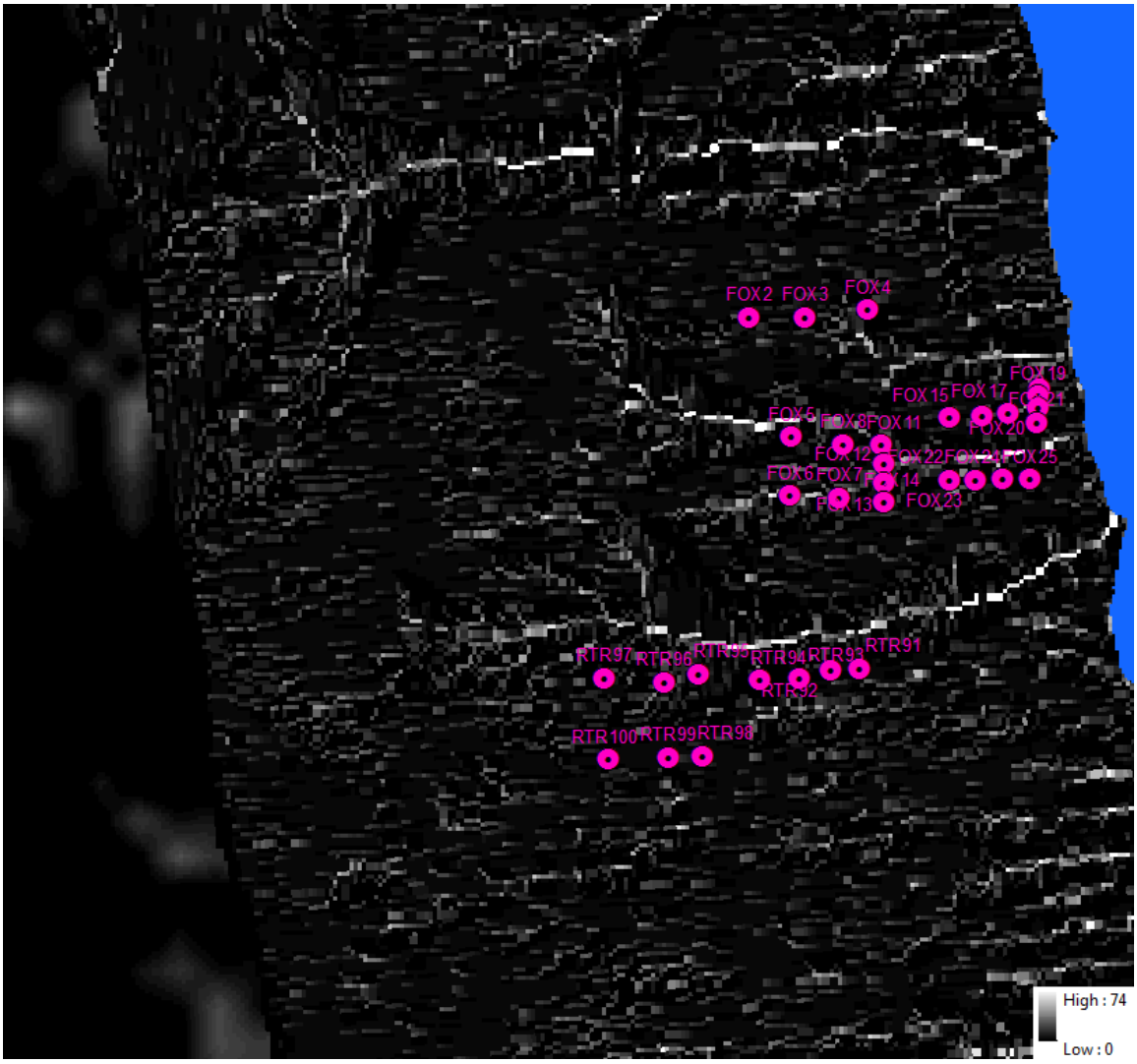

Figure 50- Close up of the flow accumulation map near Fox Run and Red Tail Ridge vineyards. Accumulation within 2km of each lake was run at a 10m resolution, while areas farther than 2km were run at 100m resolution to significantly decrease processing time.

The resulting accumulation grids ranged from values of 0, meaning no cold air would flow into the cell, to a value of 74. As with the temperature frequency values, these flow accumulation values were split into three classes. Values from 0-24 were classified as having a low risk for the accumulation of cold air and thus a low damage potential. Values between 25-49 were classified as a having some risk, while values between 50-74 were classified as having a high risk. The high risk areas were coded

with a 0, the low risk areas with a 2 and all others with a 1, using the same notation as before. The vast majority of the region was classified as a low risk (Figure 51).

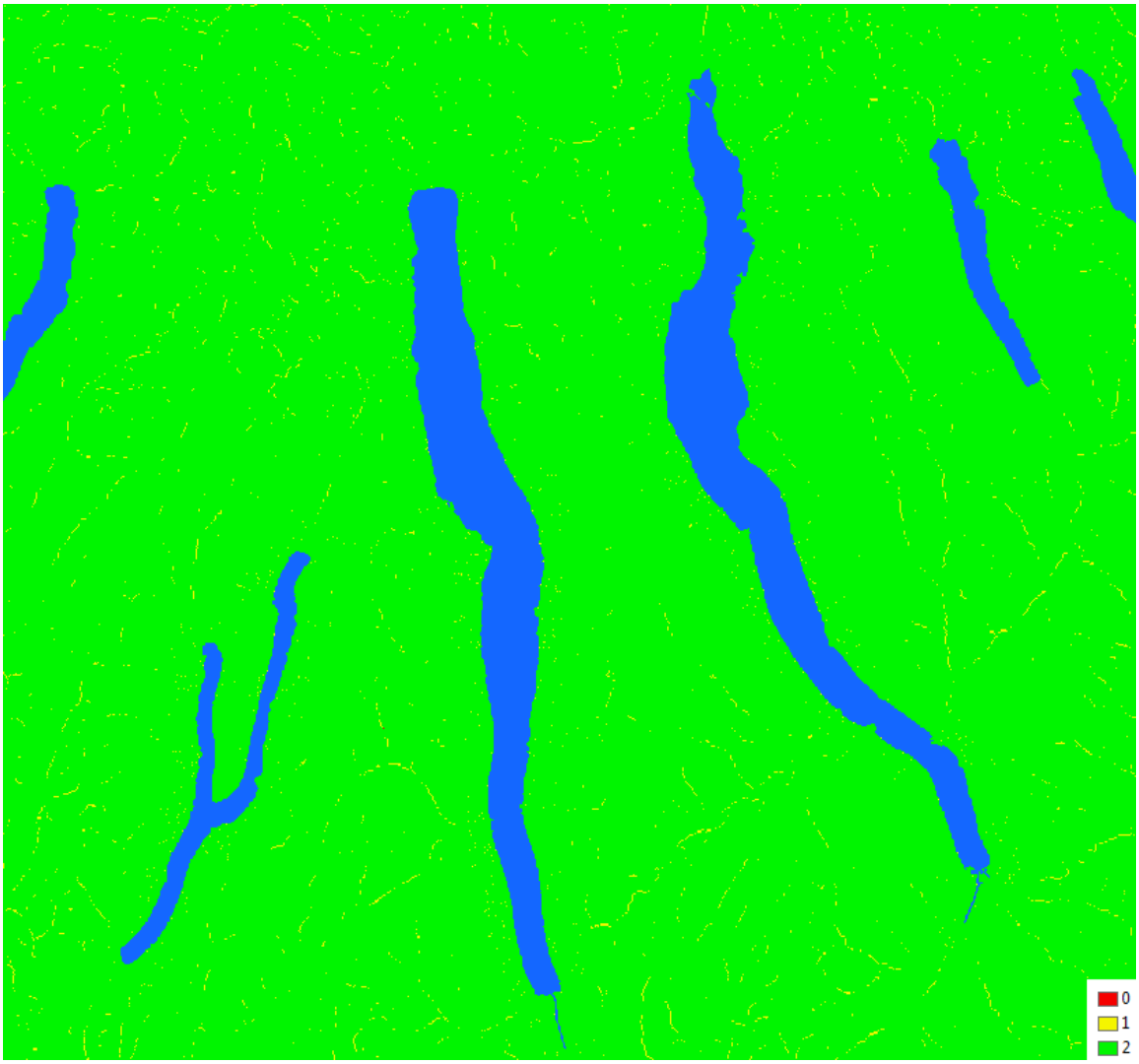

Figure 51- Flow accumulation classes over the Finger Lakes. The vast majority of the region is classified to have low flow accumulation, as shown in the green shading.

These two maps, the temperature classification and flow accumulation classification, were then combined to make a single, overall risk value, again ranging from 0 (high) to 2 (low). Areas that were classified as a high risk in either the temperature or flow classifications were coded with a 0 to keep the high-risk designation. Any other areas that had a medium risk classification in either of the maps

were coded with a 1, while a 2 was coded only if a given location was classified as a low risk in both of the analyses (Figure 52).

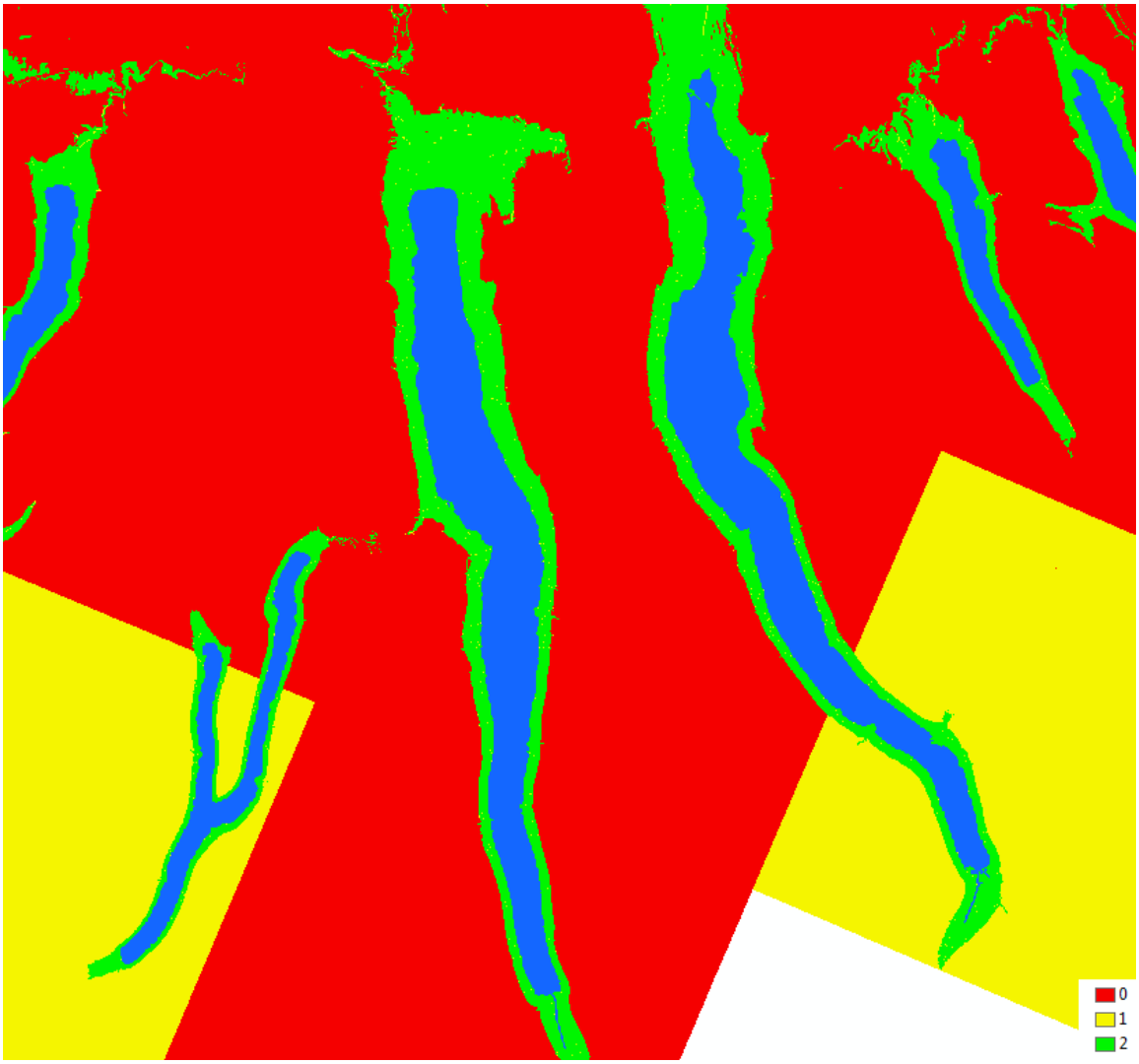

Figure 52- Final viticulture suitability classification map showing areas most suitable for viticulture (green) and areas least suitable (red) for new viticulture.

Results and Discussion

Biases

Both the NARR dataset and Lakso sensor data were subjected to testing for biases. However, one obvious bias that has a major impact on this study is the fact that all Lakso sensors are located within areas of active viticulture. There are no sensors in locations where viticulture is not ongoing, so there are no data from areas that may not

be suitable for viticulture. With the many microclimates of the Finger Lakes region, it is conceivable that distinct climate differences were missed due to sensor location. Since the goal of this study was to determine those areas that are best suited for viticulture, this is a flaw in the placement of the Lakso sensors, an activity that was conducted before this project was conceived.

To verify the temperature readings of both the NARR and Lakso sensors, additional data were obtained from the Ithaca Cornell University climate station, located on Game Farm Road in Varna, NY. This coop station, ID 304174, has a temperature and precipitation record dating back to 1893.

To investigate any potential bias in the Lakso sensors, 5 of the sensors were placed at the Ithaca station. These sensors were unfortunately not available for placement in the winter months. Instead, a data set was collected from May 10 to October 16, 2013. Three of the sensors were placed on a guy line 2m off the ground in the southeast corner of the station, similar to the placement on trellis wires in the vineyards. Coincidently, a wild grape vine grew along the guy line, further simulating vineyard conditions. The two other sensors were placed within the Stevenson screen as a test whether the PVC pipe radiation shields on the sensors were adequate.

The temperature at each hour was compared to the average temperature recorded by the preexisting data logger within the Stevenson screen, which was only available as a minimum and maximum temperature for each hour. A median difference was calculated for each sensor. The three sensors on the guy line had median biases of -0.28°C, -0.47°C and -0.67°C, indicating that the vineyard sensors recorded lower temperatures than the Stevenson data logger. Likewise, the two sensors within the

Stevenson screen were colder, with medians of -0.61°C and -0.69°C. The median of all differences across all 5 sensors was 0.53°C (Figure 15).

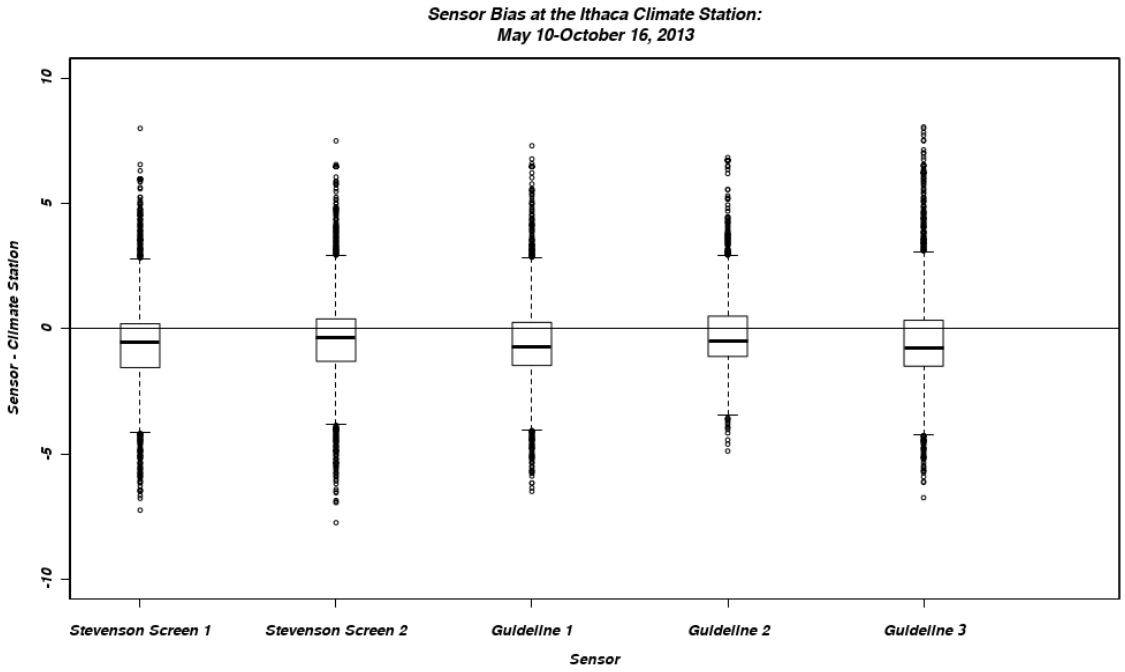

Figure 53- Hourly temperature differences between test sensors and the Ithaca Climate Station between May 10 and October 16, 2013.

There are some slight differences between the sensors on the guy line and sensors within the Stevenson screen, with the sensors within the screen appearing slightly lower. However, due to the lack of sensors, the variability among the 5 sensors, and the fact that the coldest of the guy line sensors was so similar to the two sensors within the screen, it was determined that any bias from the PVC radiation screens was minimal and not important for the purposes of this study.

Similarly the NARR dataset of 2m temperatures at the grid cell containing the Ithaca station was obtained for the May 10-October 16, 2013 time period. A similar comparison was made between the NARR and average hourly temperature of the Ithaca station. The only difference between this analysis and the aforementioned sensor

bias analysis is that the 3-hour time step of the NARR reduced the number of comparisons by one-third. The median difference over this time period was -0.29°C, representing a cold bias in the NARR data set. Compared to the sensors, the NARR temperatures were higher than all but one sensor, which had a similar median of -0.28°C (Figure 16).

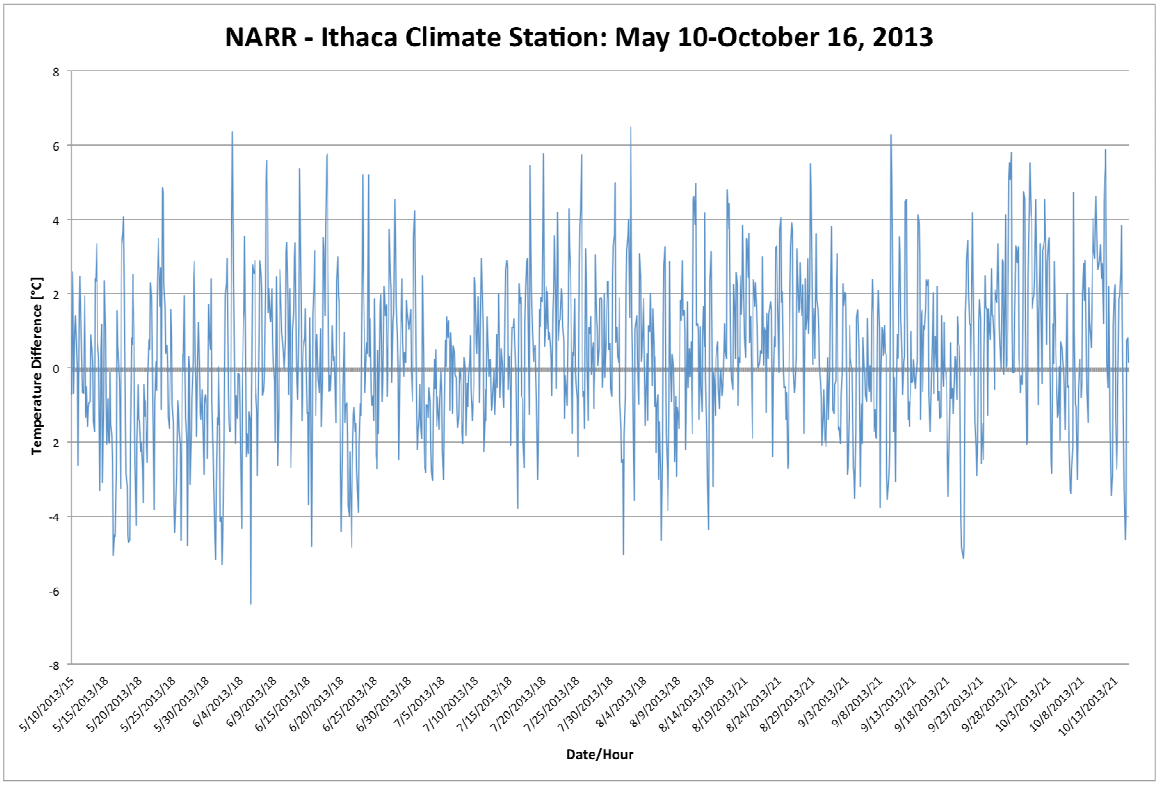

Figure 54- Difference in temperature between the NARR and Ithaca Climate Station between May 10-October 16, 2013.

A third analysis was conducted, again with the NARR and data logger within the Stevenson screen at the Ithaca station. This time, the analysis was conducted for the study time period, that is, January, February, March and December 2006-2011, excluding December 2011. All other analytical conditions remained the same. This time, the NARR data set had a bias of +0.63°C, representing a higher temperature bias in the NARR data set relative to the Stevenson data logger at the Ithaca station (Figure 17).

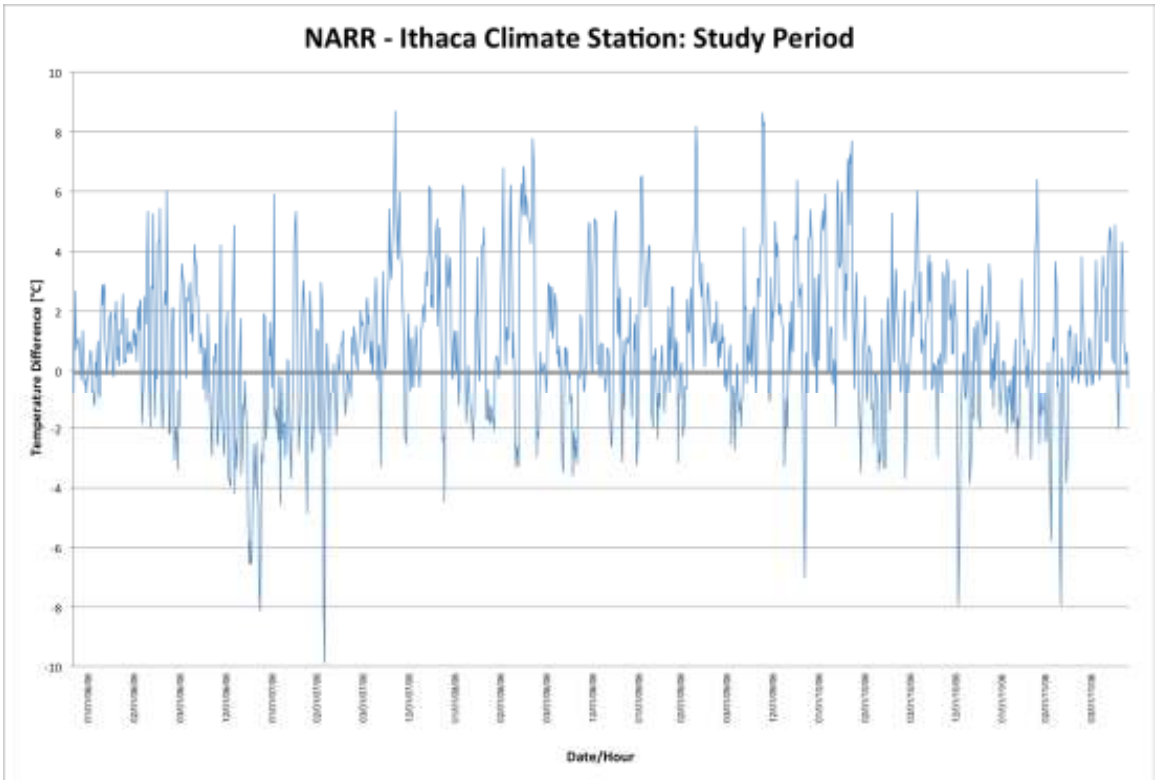

Figure 55- Difference in temperature between the NARR and Ithaca Climate Station during January, February, March and December 2006-2011 (excluding December 2011).

In the end, due to the vast differences in NARR bias between summer and winter months, it was decided that a single NARR bias value would be used for each individual month. These biases were calculated as the median temperature difference between the NARR minimums and all sensor minimums for a given month (Table 2).

Table 2- Table showing the temperature subtracted from the sensors during each month to account for bias.

Month	Bias Removal From Sensors (°C)
January	-3.39
February	-3.85
March	-2.58
December	-2.25

Comparison of Predicted Suitability & Current Distribution of Vineyards

The results of this analysis show favorable locations for all vineyards near the lakes within the Finger Lakes region, but marginal or unfavorable conditions away from the lakes at a coarse spatial scale. At a finer spatial scale, where downslope flow intersects lines of trees or vegetation, cold air can pool and cause significantly colder temperatures which may be unfit for viticulture. Dues to the fine spatial scale and lack of appropriate geospatial and climatological data at that scale, vineyard suitability modeling could not be conducted.

When comparing the results of the model to the locations of established, successful vineyards, some stark differences become apparent. In areas that were classified as unsuitable, successful viticulture is ongoing, as shown in Figures 56 and 57, which indicate locations where numerous existing, successful vineyards are located within areas classified as least suitable. However, the type of grape grown in each vineyard was not available. In consultation with Dr. Lakso, it is suspected that many of the vineyards located within the red, unfavorable areas may be primarily native and hybrid varieties of grapes, which have a higher tolerance to cold.

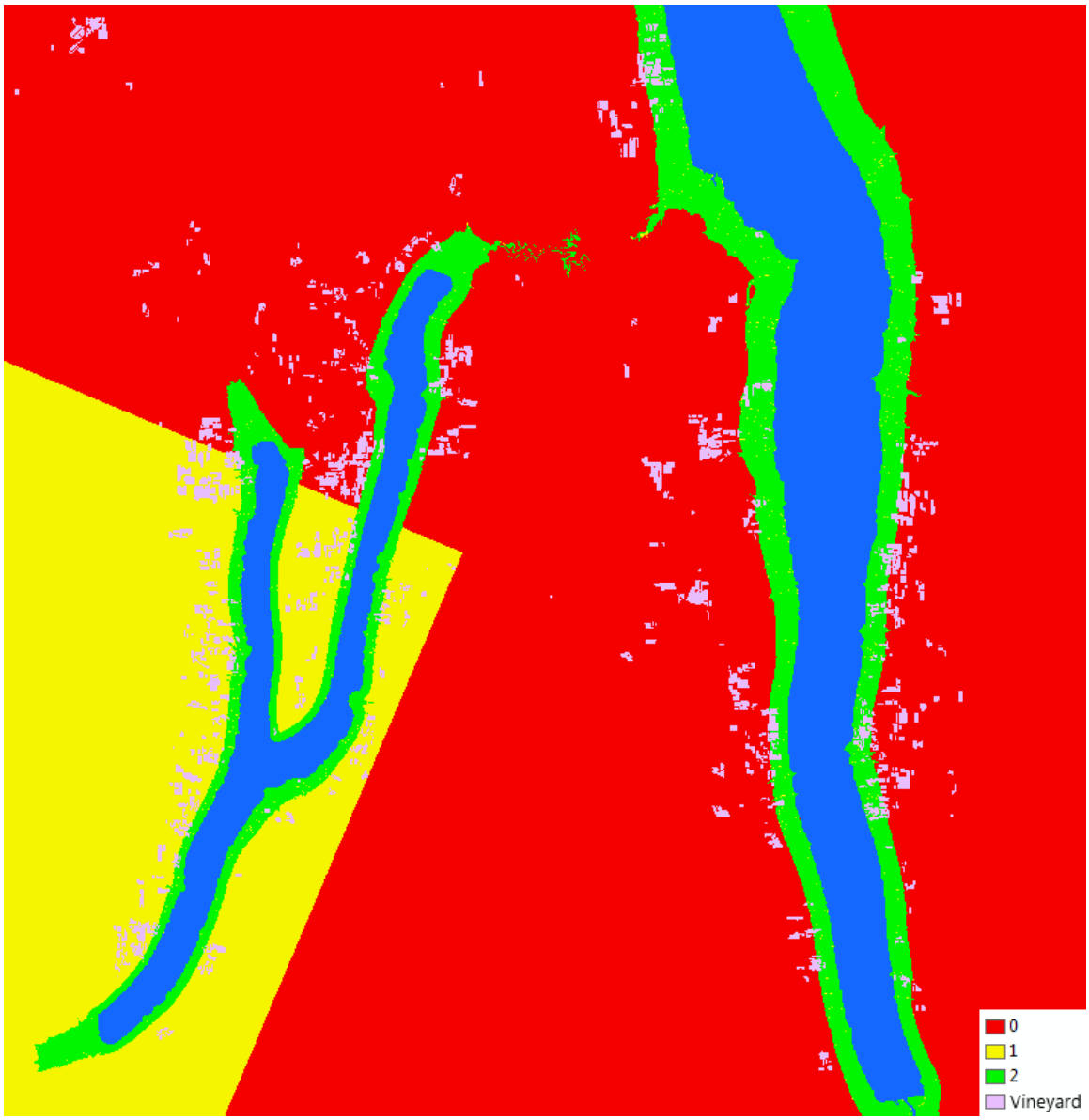

Figure 56- Close up of the viticulture suitability classification around Keuka Lake and southern Seneca Lake, with existing vineyards shown in purple. Note that many of the vineyards are located in the least suitable category may be growing hybrid or native varieties which are hardier.

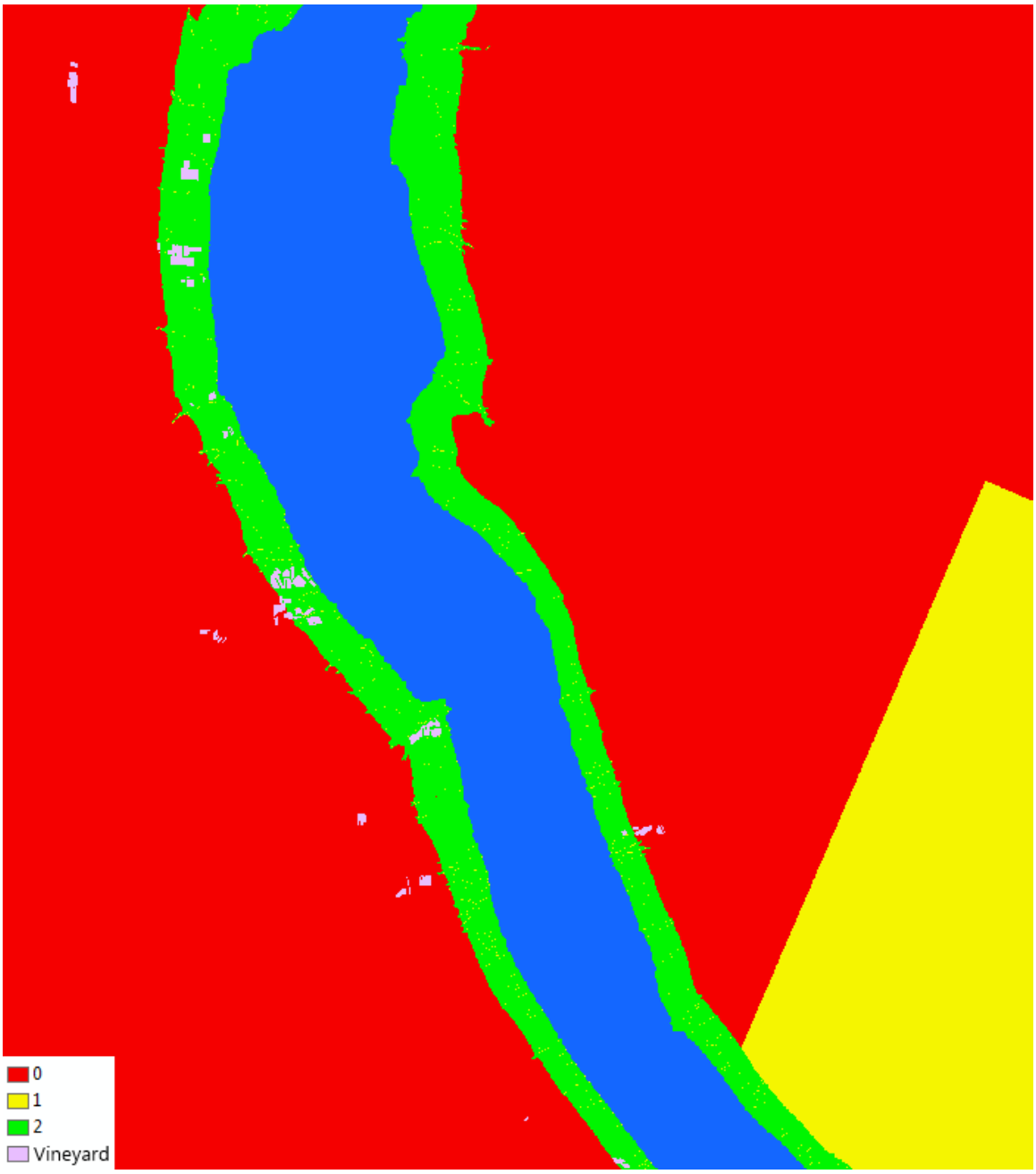

Figure 57- Close up of the viticulture suitability classification around central Cayuga Lake, with existing vineyards shown in purple. Note that many of the vineyards are located in the least suitable category may be growing hybrid or native varieties which are hardier.

More discrepancies can be seen in Figure 58, which shows sensors RTR 97 and RTR 100 in the least suitable classification, while RTR 95 is in the most suitable classification. However, sensor RTR 95 consistently measured colder tmperatures than

either of those sensors. This is just one example of a number of differences seen in the climate maps produced by the model.

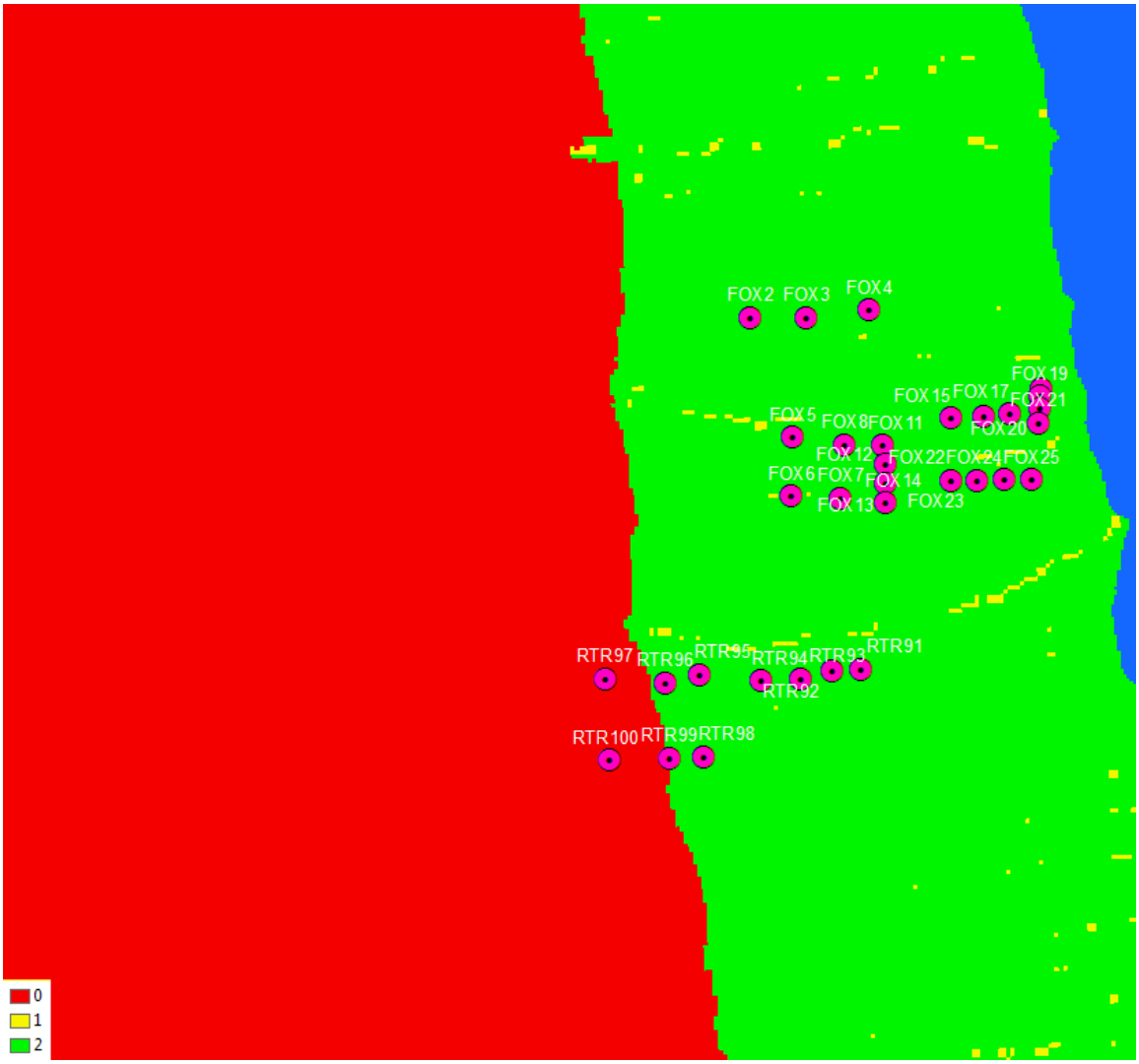

Figure 58- Close up of the viticulture suitability classification near Fox Run and Red Tail Ridge vineyards. Note that sensors RTR 97 and 100 are both classified as least suitable, while RTR 95, one of the coldest sensors, is in the most suitable category. Additional research using improved sensor locations would significantly improve vineyard suitability classification and mapping.

Summary & Conclusions

Key Findings

This research produced some key findings that are worth noting. Primarily, the presence of tree lines intersecting downslope air flow could result in the pooling of cold air and could drastically increase the risk of damaging cold temperatures in the area of

the tree line. Furthermore, the establishment of a tested process for quantifying the influence of the Finger Lakes on the temperature of the surrounding land will allow further research into the microclimates of the Finger Lakes to the direct benefit of viticulture in the region.

Future Research

It is recommended that this study be replicated with a new sensor data set. Sensors should be placed strategically after extensive geographic analysis is conducted. Recommended sensor locations include areas far from the lake, where lake modified air is minimal or absent, in areas where viticulture is not practice, near tree lines, in frost pockets and in other areas of varying terrain. By replicating this study with improved sensor locations, a much more accurate map of viticulture suitability could be produced. For a more accurate verification, knowing the varieties of grape grown within a certain vineyard is vital and it is highly recommended that such a data set be compiled.

REFERENCES

Chung, U., Seo, H., Hwang, K., Choi, J., Lee, J., and Yun, J., 2005: Minimum temperature mapping over complex terrain by estimating cold air accumulation potential, *Agricultural and Forest Meteorology*, 137, 1-2, 15-24.

Fingerlakes.com, 2014 [available online at http://www.fingerlakes.com/seneca/seneca-lake-wineries].

Fliegel, Myron H., 1973: Temperature Measurements and Internal Waves in Seneca Lake, New York. Office of Naval Research Advanced Research Projects Agency Technical Report #9, 149 pp [available online at http://www.dtic.mil/dtic/tr/fulltext/u2/769227.pdf].

National Center for Environmental Protection, 2007 [available online at http://www.emc.ncep.noaa.gov/mmb/rreanl].

Newman, J., 1986: Vines, Wines, and Regional Identity in the Finger Lakes Region, Geographical Review, **76**, 3, 301–316.

New York Vineyard Site Evaluation System , 2014 [available online at http://arcserver2.iagt.org/vll/learnmore.aspx#Climatemap].

Pagay, V. and Cheng, L., 2010: Variability in Berry Maturation of Concord and Cabernet franc in a Cool Climate, *American Journal of Enology and Viticulture*, **61**, 1, 61-67.

Wine Institute, 2010 [available online at http://www.iwineinstitute.com/avabystate.asp].